Alma Mater Studiorum- Università di Bologna

SCUOLA DI SCIENZE

Dipartimento di Chimica Industriale"Toso Montanari"

Corso di Laurea Magistrale in

Chimica Industriale

Classe LM-71 - Scienze e Tecnologie della Chimica Industriale

Synthesis of mesoporous zeolites for the selective conversion of sugars into methyl lactate and other hydroxyesters.

Tesi di laurea sperimentale

CANDIDATO

Annalisa Sacchetti

RELATORE

Chiar.mo Prof. Fabrizio Cavani

CORRELATORE

Irene Tosi

Anno Accademico 2017-2018

Index

1. Introduction 4
1. 1 Zeolites 5
1.1.1 Shape selectivity 6
1.1.2 Zeotypes 8
1.1.3 Hierarchical zeolites 10
1.2 Biomass as a source for polymers 15
1.2.1 Carbohydrates 17
1.2.2 From glucose to lactic acid 20
1.2.3 Zeolites for biomasses conversion 21
2. Aim of the project 27
3. Materials and methods 27
3.1 Synthesis of microporous catalysts with high Lewis acidity 28
3.2 Synthesis of mesoporous catalysts 29
3.2.1 Desilication 29
3.2.2 Surfactant templating on a Sn-zeolites 30
3.2.3 Surfactant templating on a H-zeolites 30
3.2.4 Dissolution-Reassembly procedure 31
3.2.5 Hydrothermal synthesis with PDADMA 31
3.2.6. Hydrothermal synthesis with PDADMA and TEAOH 31
3.3 Reactivity 32
3.3.1 Reaction conditions 32
3.3.2 Analysis of products mixtures 33
3.4 Catalysts characterization 34
3.4.1 Composition properties: XRF 34
3.4.2. Structure properties 35
3.4.3 Surface properties 37
3.5 Recovery test 38
3.6 Catalytic tests with other substrates 38
4. Results and discussion 39
4.1 Characterization of catalytic systems 39
4.1.1 Structure analysis- XRD 41
4.1.2 Acidity evaluation- XRF and TPD 45
4.1.3 Pore size analysis- BET 46
4.2 Conversion of glucose using different microporous zeolite frameworks 48
4.3 Recovery tests 53
4.4 Activity of mesoporous zeolites for the conversion of glucose 53
4.5 Activity of the catalytic systems for the conversion of bulky substrates 55
4.5.1 Catalytic tests on inulin 55
4.5.2 Catalytic tests on sucrose 59
4.5.3 Catalytic tests on cellobiose and maltose 61
4.5.4 Catalytic tests with starch 64
5.Conclusion 65
6. Appendix 66

6.1 Appendix A – XRF data- Si/Al and Si/Sn ratio. 66
6.2 Appendix B – NMR spectra 67
6.3 Appendix C- SEM pictures 69
7.References 72
8. Acknowledgements 76

1. Introduction

During the last decades petroleum has been the main feedstock for the production of the majority of fuels and chemicals, but the limited cheap supply of the so-called “black gold” has pushed the research to focus in renewable and sustainable resources. Indeed, chemical products can be obtained both from oil and more sustainable starting material likewise biomasses. This latter pathway often presents more obstacles due to the big amount of by-products and side reactions that can overcome and the lack of existing technologies.

Catalytic routes are therefore necessary in order to make these alternative-starting materials competitive with the already well-established petroleum.

Again, studies and discoveries that have been done for he use of fossil feedstock, can be applied for renewable resources. For instance zeolites, which are widely used in cracking processes, find novel and promising applications when it comes to biomasses.

In this work the attention is pointed out on six-carbon atoms sugars as renewable starting materials. Using Lewis acidic zeolites, it is possible to convert them into methyl lactate and other important functionalized molecules, which can be used as building blocks for the production of bio-polymers.

Changing the pores size and the framework of zeolites, it is possible to investigate the selectivity regarding different products of interests.

In the first part of the project diverse frameworks of zeolites have been synthesized and tested for the conversion of glucose.

Subsequently, it has been investigated the possibility to create mesopores systems as catalyst and test their selectivity for the conversion of substrates larger thank glucose In fact, while in most cases the microporosity inside the zeolite is suitable for cracking applications, diffusion limits overcome using bigger molecules, such as polymers.

1. 1 Zeolites

Zeolites are crystalline microporous aluminosilicates consisting of a network of SiO_4 and AlO_4. Their primary structure is a tetrahedron TO_4 where T is mostly Si or Al and the oxygen atom in shared between two tetrahedral building units. This interconnectivity leads to a 3D structure and presence of channels and pores[1].

Even if many zeolites exist in nature, a large number have been prepared synthetically. In fact more than 170 different structures have been characterized so far and several new types still appear every year.

The International Zeolite Association (*IZA*) deals with their classification using a 3-letter code for each framework, and ranks all the zeolites, providing information on their main proprieties (e.g cell parameters, framework density, pore size, diameter etc.).

As the Table 1 shows, each structure can be defined according to the pore size in macroporous, mesoporous and microporous. Typically, original zeolite pores have diameters in the range of 4–12 Å and they are therefore called micropores according to the IUPAC classification of porous materials[2].

Pore size (Å)	**Definition**	**Ring size**	**Pore diameter (Å)**	**Example**
> 500	Macroporous			
20-500	Mesoporous		15-100	MCM-41
< 20	Microporous			
	Ultralarge pore	20	6.0 x 13.2	AET
	Large pore	12	7.4	FAU; BEA
	Medium pore	10	5.3 x 5.6	ZSM-5
	Small pore	8	4.3	CHA

Table 1: Ranking of different zeolite according to their pore dimension[3].

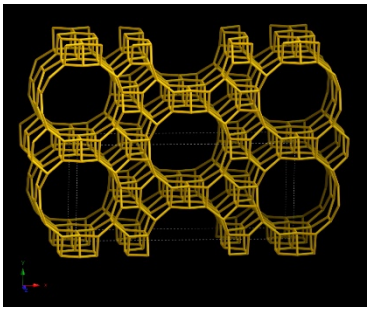

AET: $AlPO_4$-8

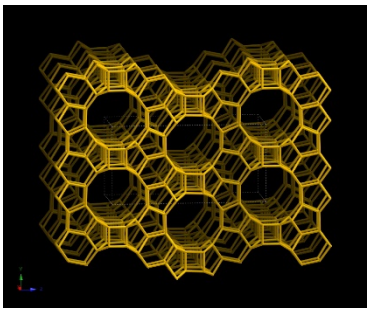

BEA

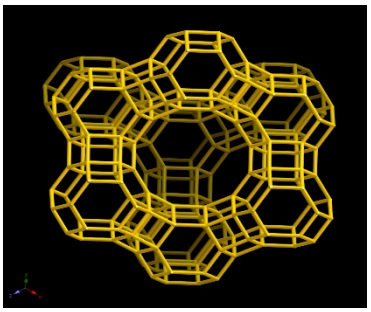

FAU

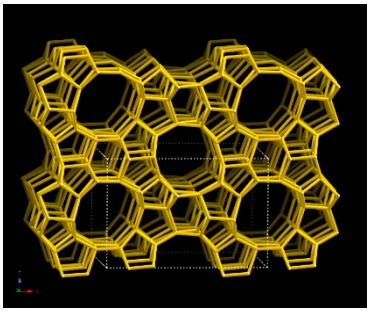

MFI:ZMS-5

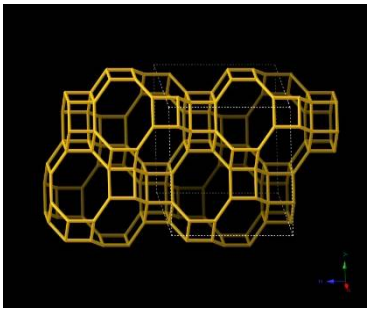

CHA: SAPO-34

Figure 1: Examples of different zeolite frameworks.

1.1.1 Shape selectivity

The presence of pores with specific and uniform size makes zeolites unique materials; they act as molecular sieves, being able to allow or avoid different reactions pathways according to the size of the molecules involved.

The concept of shape-selectivity was introduced in 1960 by some researchers from *Mobil* who observed the size-dependent catalytic performance of zeolites in cracking reactions.[4]

Generally there are three different type of shape selectivity: towards reagents, transition state and products[5]. This is one of the main aspect that allowed great applications of zeolite in catalysis, it permits to increase the selectivity of a product reducing undesired intermediates or by products as the figure 2 shows:

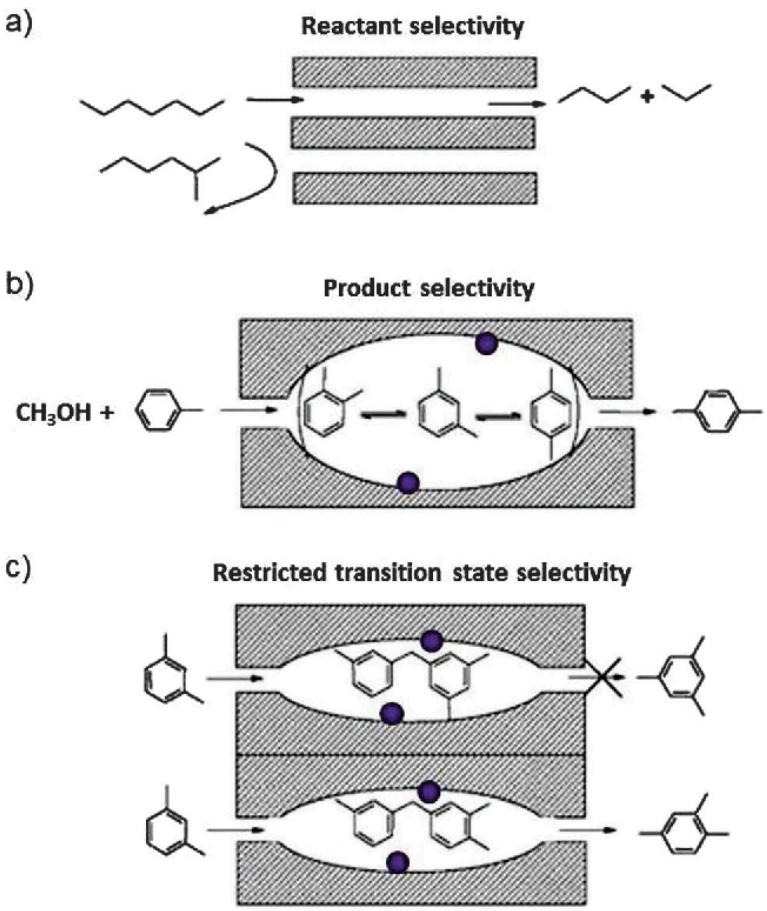

Figure 2: Representation of different types of shape selectivity made by a zeolite .

Similar concept can be applied to biomasses sources. An example of reagents selectivity is given by sugars: hexoses are not able to isomerise to five carbon ring molecules over Sn-MFI (medium pores) while the reaction is successful over Sn-BEA (larger pores). Trioses instead, are able to enter the Sn-MFI cavity and can then be converted[7].

1.1.2 Zeotypes

As mentioned before the framework of zeolites is made of Si-O-Si and Al-O-Si bonds, which occurs repeatedly over the space (Figure 3).

The presence of $[AlO_4]^-$ in the framework, instead of SiO_4, generates a negative charge, which can be balanced by external cations. These can be H^+, NH_4^+,Na^+or redox-active ions such as Fe(III), Cu(II), Co(II), or Ag(I). According to the different cation, the zeolite has ion-exchange capacity or redox activity. This first property revealed to be very useful in processes like water deionization[8] and detergents production.

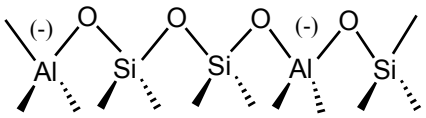

Figure 3: Representation of the internal Si-O-Al bond inside the structure

If a proton balances the negative charge, the zeolite in solution acts as Brønsted acid, which means that is able to donate H^+: this property is enhanced with a decrease of Si/Al ratio in the structure.

Zeolites can also have Lewis acidity charachter, mainly given by extra-framework aluminum, which is not tetrahedrally coordinated inside the framework. However in natural zeolite this intrinsic Lewis acidity is weaker than the Brønsted acidity.

The increase of the Si/Al ratio, which involves a lower amount of Aluminum inside the framework, can be favorable in many cases.(for instance, it improves the hydrothermal stability of the zeolite). The removal of Al from the framework allows the creation of vacant sites and the possibility to introduce subsequently metals with major Lewis acidity proprieties[9].

In fact zeolites are not only aluminosilicates: the Al (III) cation can be substituted by other metals (Fe, Ge, Sn, Mn, Ga, etc.) giving a variety of different metallosilicates[10,11,12]identified as zeotypes. Introducing specific metals like Sn, Ti or Zr it is possible to increase the Lewis acidic proprieties, making the zeolite able to attract and accept electrons.

The result is therefore a catalyst which posses both relevant Brønsted and Lewis acidity. This latter propriety has given good results for the conversion of biomass-derived sugars, as will be discuss afterward.

1.1.2.1 Synthesis of Sn-zeotypes

Bottom-up – hydrothermal synthesis

Corma *et al*. proposed a hydrothermal synthesis to obtain high active Lewis acidic zeolites, with the direct incorporation of the metal during the treatment [13]. The conventional hydrothermal method involves mixing a silica and aluminum precursor with a structure-directing agent (SDA), which leads to the formation of the zeolite framework. After the introduction of a mineralizing agent (often HF) the mixture is treated at elevated temperatures and autogenous pressure for long periods. In the Corma procedure the initial amount of Al is significantly lower than the usual amount and the Sn precursor tin(IV)chloride is added in the first part of the synthesis. One of the main advantages of this technique is the achievement of highly-defect free crystals.

However, the involvement of HF as mineralizing agent makes this synthesis less easy to apply on industrial scale due to environmental and safety limitations. Moreover the presence of large Lewis acidic centres (like Sn^{IV}) leads to a retardation of the zeolite nucleation, which results in longer timescales (up to 40 days) and obtainment of unwanted large crystals (>1 μm)[15].

Top-down method – dealumination and metal incorporation

The top-down synthesis start from commercially available zeolites, with subsequent removal of framework aluminium and insertion of the desired metal. There are several routes for this procedure, which can be classified in two main groups based on the method used for the removal of the aluminum: the first uses chemical agents, as mineral acids, and the second steam and thermal treatments at 600-800°C [14]. The contact with steam causes the hydrolysis of Al-O-Si bonds and a subsequent expulsion of Al from the framework.

Regarding the acidic treatment, the parental zeolite is treated with a defined amount of acid, at a settled temperature, and the hydrolysis of the Al-O-Si bonds occurs. This technique ensure a

quantitative Al extraction as C. Hammond et al. proved[15], avoiding the presence of extra-framework aluminum (EFAL) which can interfere with catalytic proprieties.[16]

However the impossibility to monitor and limit the amorphisation of the crystalline structure caused by the acidic treatment is one of the main drawbacks of this approach. Nevertheless, adjusting treatments conditions, it is possible to avoid significant alterations of the framework[5].

Once that the hydroxyl nests are created inside the zeolite as a result of the aluminum displacement, the requested metal can be introduced in a variety of ways. These include wet impregnation,[17,18,19] gas-phase grafting [20,21], solid state ion exchange (SSIE) [10,12,23] or reflux impregnation.

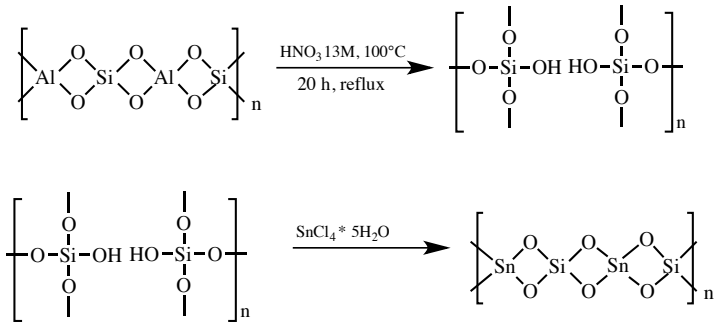

Scheme 1: Procedure for the dealumination and Sn impregnation of a zeolite[11]

Some factors, as the presence of defects and residual aluminum inside the zeolite, can cause an incomplete incorporation of metal inside the cavities, and subsequent formation of the metal oxide form [24] which is catalytically inactive. Taking into account that this inconvenient can be related to the impregnation method or utilization of big excess of metal precursor, it can be avoided or limited and make this preparation method straightforward and easily applicable.

1.1.3 Hierarchical zeolites

The microporous structure is the key feature for a high selectivity in many reactions but at the same time imposes significant diffusion limitations on large molecules leading to a lower efficiency of the catalytic system in the conversion of bulky substrates. The diffusivity towards the active site is often the rate-determining step (RDS) of a reaction catalyzed by a

heterogeneous system, especially when reagents molecules match the size of the pores. This can happen when dealing with micropores (diameter < 20 Å): a sharp decrease in the molecular diffusivity to orders of magnitude is observed when the pore diameter passes from 100 nm to lower than 1nm[25] (Fig. 4). As a consequence, reagents can't reach the active site properly, affecting negatively the yield of the reaction.

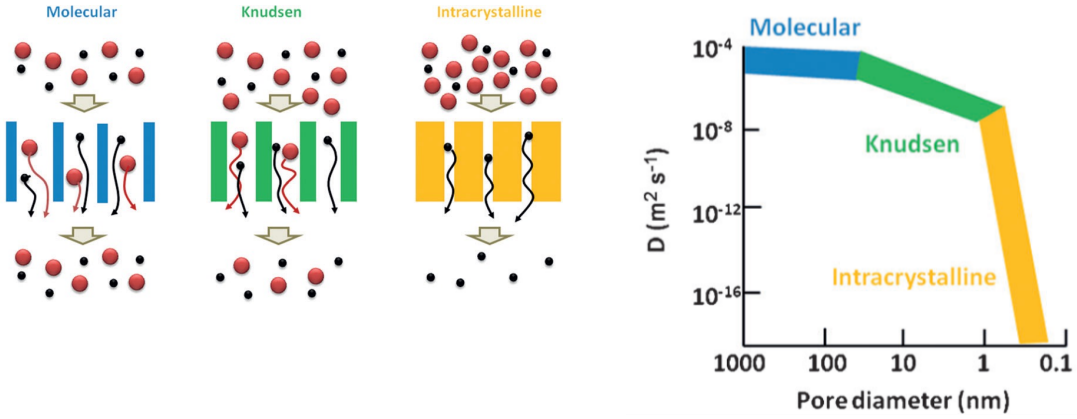

Figure 4: Schematic representation of pore size effect in the diffusion (D) of large (red) and small (black) molecules [18]. On the right is reported the dependence of the diffusion rate from the pore diameter.

In the last decades great efforts have been done in order to overcome the diffusional issues and once more, the possibility to tailor the zeolite framework aids to reduce diffusivity limitations. In fact it is possible to create a second level of porosity inside the cavity: the new catalysts can have therefore mesopores (2-50 nm) or even macropores(>50 nm) in accordance to the engaged synthesis strategy .

In many cases it is observed an improvement in catalytic performance of hierarchical zeolites over the classical ones[26]. Besides the increase in the rate of diffusion other advantages can be achieved:

1) Reduction of the steric limitations for converting bulky molecules.

   Since the secondary porosity is not expected to do be sterically hindered, the active site may catalyze reactions that involve big molecules, widening the range of zeolites applications.

   Moreover, starting from the same reagent, the selectivity towards products can undergo variations: bigger pores can allow the formation of bulkier transition state molecules, leading to a more spread products composition compared to the microporous systems.

2) Decrease in the coke deactivation.

The formation of carbon coke is present in all the reactions that involve organic compounds[27]. It consists in the formation of heavy by-products, which form a deposit on the surface, causing deactivation of the catalyst. The coke can accumulates both inside and at the entrance of the pore, hindering the pathway of the molecules inside the active site. However it is important to take into account that the coke finds a wider pores volume to fill in hierarchical materials than in microporous systems. The result of these two effects is that usually a larger amount of coke is formed, but it leads to lower deactivating effects compared to conventional zeolites[28,29].

1.1.3.1 Preparation strategies of hierarchical zeolites

The formation of mesopores inside the framework can be achieved following two different pathways:

- *Bottom-up method,* or primary synthesis, which involves the use of templates and structure directing agents (SDA);
- *Top-down method*, or post-synthetic modification of a parental zeolite.

"Bottom-up method"

This procedure involves the crystallization of the zeolite using a template, which at the end of the coagulation is removed by calcination or acidic dissolution, leading the formation of mesopores.

The templates involved can be divided into two categories:

- Hard templates, including all the carbonaceous materials (e.g carbon fibers, nanotubes, particles), carbon aereogel and polymers (e.g polystyrene , polyurethane) and some inorganic guides as silica or $CaCO_3$.
- Soft templates concerning cationic surfactants like cetyltrimethylammonium bromide or chloride (CTAB or CTAC), mesoscopic cationic polymers, organosilanes, starch, bacteria and others [30,31].

Recently Xiao et al.[32] have presented a hydrothermal synthesis using cationic polymers and it appears to be promising for more green and environmental friendly solutions.

One of the most significant advantages of the " bottom-up" approach is that the degree of mesoporosity can be increased without compromising some features that characterize the zeolite e.g: Si/Al ratio, crystalline structure, physical proprieties etc. Even more it is possible to tailor the pore in accordance with the dimension of the employed surfactant.

"Top Down" method

a. Dealumination:

The dealumination, which is usually conducted for tuning the acidity of the zeolite, causes a silicon migration inside the framework, following the so-called Marcilly mechanism [35](fig. 5). It involves the silicon migration after the aluminum removal with consequent coalescence of vacancies and formation of mesopores.

However the induction of mesopores is not the primary aim of this technique but it is only a side effect, hence more suitable and reliable approaches have been developed.

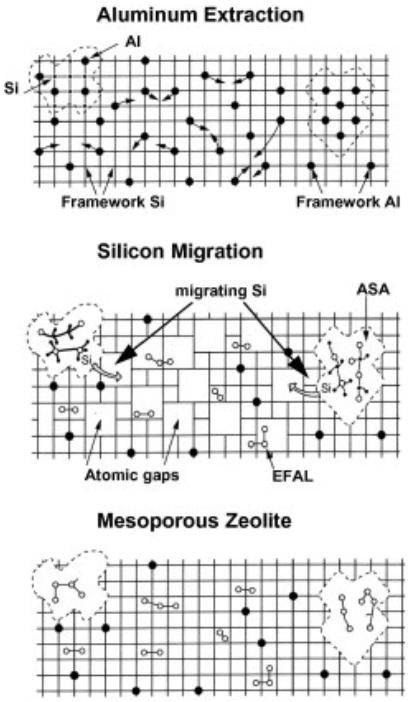

Figure 5: Marcilly mechanism rapresentation [30]

b. Desilication

Mesopores can be induced inside the parental zeolite with a process called desilication, which involves the removal of silicon from the structure.

It was first reported in 1960: Young and Linda observed that MOR zeolites can be treated with an alkali solution leading to a small leach of structural silica and improving the adsorption capacity.[36]

The initial Si/Al ratio has a great influence on the process: Groen et al. showed that a high amount of Al inside the framework (Si/Al < 20) prevents the silicon extraction, limiting the formation of pores. On the other hand, when Si is in great excess (Si/Al >50) it causes an excessive and unselective dissolution of the framework(Figure 6). Considering these two aspects they proved that a Si/Al ratio between 25 and 50 is optimal in order to obtain mesopores successfully[37].

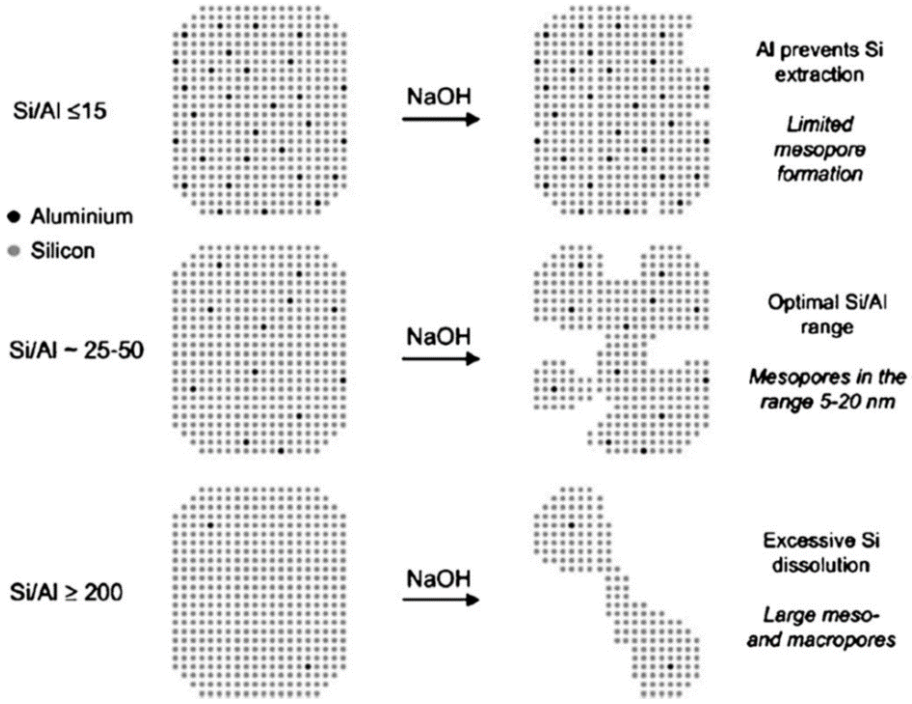

Figure 6: Schematic representation of the influence of Si/Al during desiliciation (from J.C. Groen, J.Phys. *Chem*., **2004**).

The desilication approach is very versatile because it can be easily applied to different frameworks but there are some issues associated with this method. First of all there can be significant loss of both material and microporosity due to a decrease of the zeolite crystals caused by the silica leaching. Even more the introduced mesoporosity is hardly controllable in its homogeneous and size distribution.

c. Surfactant templating

Martinez et al. reported that cetyl trimethylammonium bromide (CTAB) molecules can actually enter the zeolite through its microporosity. Once inside the surfactant molecules self-assemble to produce micelles, which are responsible of the formation of mesopores [38] (Figure 7).

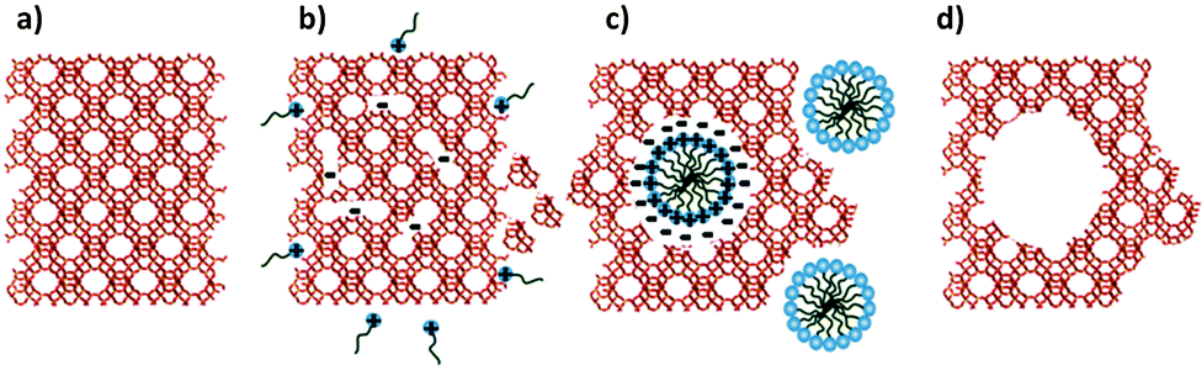

Figure 7: Proposed method for the formation of mesopores with the surfactant-templating approach: a) Original commercial zeolite; b) Si-O-Si bond opening and reconstruction in the basic media; c) rearrangement of the surfactant into micelles and re-organization of the zeolite structure; d) removal of the surfactant by calcination and formation of mesopores (from ref. 39 *Catal. Sci. Technol.*, 2012) [39].

d. Dissolution and reassembly procedure

Goto et al.[40] in 2002 and later Ivanova et al.[41] in 2004 proposed a new process, which involves two steps: an initial partial or complete destruction of a commercial zeolite, followed by a hydrothermal treatment with CTAB and NaOH. In the proposed mechanism the dissolved zeolite species are re-condensed and re-assembled around the surface of the surfactant, rising the final formation of mesopores. Two levels of mesoporosity are observed: the well-controlled mesopores originated by the surfactant, and the irregular ones created during the first step on the remaining zeolite.

The surfactant-templating process presents some important advantages, allowing the formation of tailored mesopores in a given zeolite, preserving its key properties like acidity, crystallinity and hydrothermal stability.

1.2 Biomass as a source for polymers

One of the main challenges that must be faced in present days is the employment of renewable sources for the production of those compounds that are currently derived from petroleum. This challenge involves many fields of application, and among these the polymers sector has an impactful role.

In 2015 the plastics production reached 322 Mtons, with an increase of 3-4% annually[43]. The vast majority of plastics are still derived from petrochemicals sources and are not biodegradable which make them very persistent after their use and difficult to dispose of,

concurring to the accumulation of plastics in the oceans[44,45,46]. Improvements have been done in order to minimize the issues related to their disposal: when polyolefins are sensitive to air and light they can be reabsorbed into the biological system, acquiring biodegradability proprieties.

However this approach does not act with the aim of finding a solution to the depletion of fossil reserves. In this regarding bio-plastic have to be considered since they derive from renewable carbon resources such as biomass. Biomasses can be employed for generating energy and heat by burning[47], but a better valorization of this source involves biological or chemical transformations for the production of chemical products.

In 2017, 2,05 Mtons of bioplastics were produced, accounting the 1.5% of the entire plastics production [48]. Of these, most of them were only partially bio-based, such as polyurethanes (PUR, 47 %) and polyethylene terephthalate (PET, 26 %). Polylactic acid (PLA) or polybutylene succinate (PBS) are two examples of fully bio-based polymers but constitute only the 10% and 4,9% respectively of the total amount of bioplastics produced[42] (figure 8). Despite the relatively small amount of bio-based polymers currently produced, their technical substitution over the traditional ones is estimated to reach the 90% in the future[49], and in order to move in this direction many researches have been carried out.

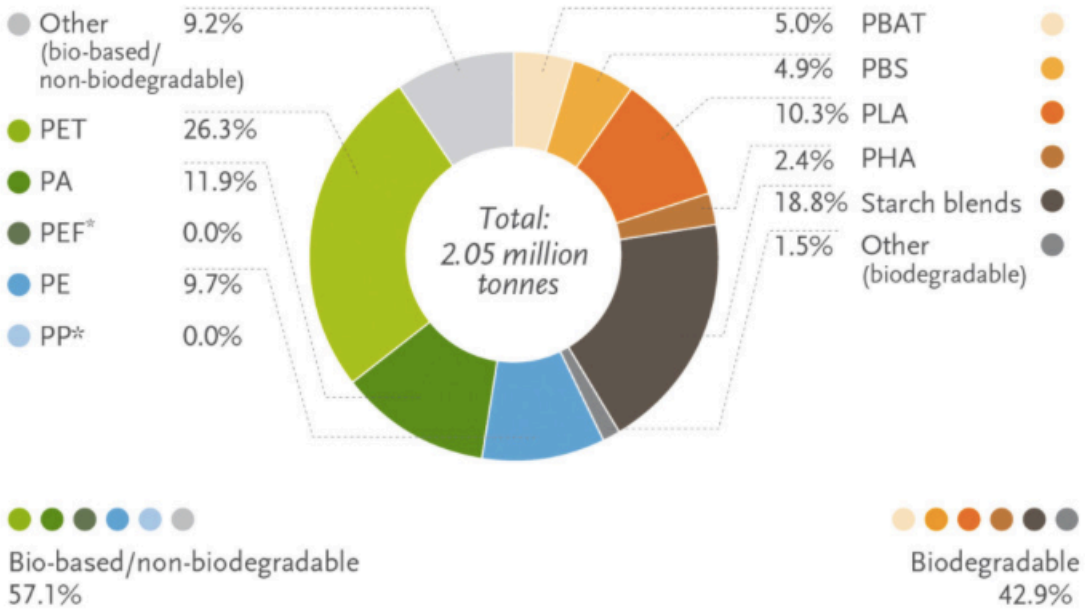

Figure 8: Global plastics production capacities of bioplastics in 2017[42].

An example of biotechnology application for bio-plastics production is represented by the *in vivo* production of polyhydroxyalkanoates (PHA): these bacterial polyesters can be isolated from the cells after a fermentative process, providing a valid substitution to conventional petrochemical routes[51].

The application on a large scale of biotechnological processes is however restricted: their limitations in term of operating conditions (temperature, oxygen concentration, time etc.) and multi-step purifications make the route not always favorable for the scaling-up. For examples fermentation are often performed in batch reactors for many days and the need of a pH adjustment causes the formation of salts, making the entire process not environmentally friendly. Moreover, the amount of products that is obtained can change from one batch to the other, making a continuative production hard.

Since biotechnological systems need an improvement in their performance, the chemo-catalysis can represent an alternative: chemo-catalytic methods can overcome some of the main issues found for enzymatic processes. They allow broader range of solvents, temperature, pressure and the possibility to tune the reaction conditions, leading to faster and transformations.

The use of enzymatic processes allows only the formation of one enantiomer of the desired compounds: catalytic systems not only permit the formation of the racemic mixture, but also the development of new molecules that would not be produced by enzymes as well as the possibility to design specific catalysts for multistep reactions.

Catalytic processes need to face some challenges as well: the optimization of the catalysts to obtain a good stability and activity is never straightforward and requires many adjustments. Especially when it is about highly functionalized molecules as biomasses, the selectivity towards the desired product plays a crucial role.

1.2.1 Carbohydrates

Biomasses can differ in the primary composition and, in most of cases they consist of functionalized molecules, representing one of the main differences from oil. The majority streams of biomasses are formed by lignocellulose, carbohydrates, lipids (containing triglycerides from animal fats), proteins and terpenes[52]. Carbohydrates constitute the predominant fraction of renewable biomass and among all the sugars, glucose and xylose are

the most available, making up an average 70% of the total carbon[22] and the protagonist of the production of a big variety of chemicals.

- Glucose

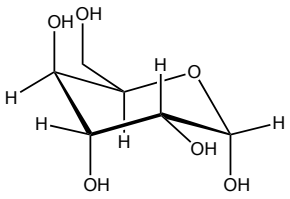

Figure 9: Glucose

Glucose is a six-carbon atoms sugar found in a wide range of disaccharides, which after hydrolysis of the glycosidic bond release the monosaccharide. Currently, the direct industrial conversion of glucose using inorganic catalysis has only been applied in the production of sorbitol and gluconic acid but several important chemicals (Figure 10) has been shown to be accesible via catalytic route, in particular the production of 5-hydroxymethyl furfural, levulinic acid, lactic acid and hydroxyesters that can be used for bio-polymers synthesis.

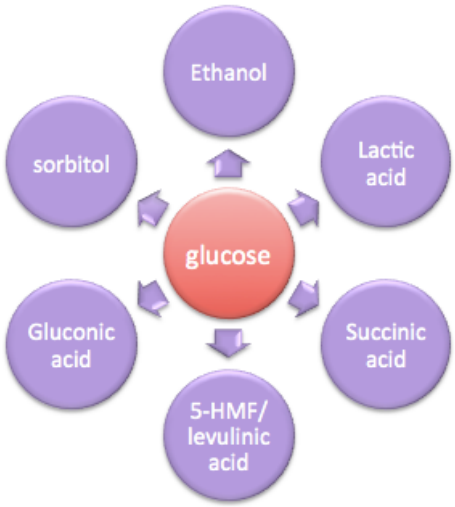

Figure 10: Some of the possible products obtained from glucose

- Fructose

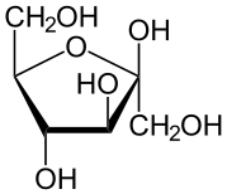

Figure 11: Fructose

Fructose is a ketonic monosaccharide obtainable from glucose by isomerization but also derived from sugar cane, sugar beets and corn. Due to the five membered ring is more reactive than glucose and, as will be discussed subsequently, once it is obtained from glucose it reacts immediately. Fructose is widely engaged in food industry as a substitute of sucrose as sweetener, due to its higher sweetness potency. In the last decade many applications have been found for it as a precursor for many chemicals like for instance the production of furanic molecules for the production of non-petroleum derived polymers.

- Sucrose

Sucrose can be refined from sugar beet or sugar cane and with a global production of more than 160 million metric tons per year represents one of the major streams of glucose [53,54].

Others disaccharides can be used as a source of glucose and fructose, widening the availability of glucose and fructose as starting material for chemicals product.

Hereafter some alternatives to sucrose are listed.

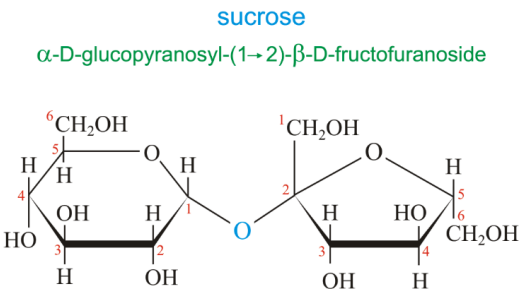

Figure 12: Sucrose

- Inulin

Inulin is found naturally in more than 36.000 species of plants like wheat, onion, chicory and Jerusalem artichoke acting as an energy reserve and as regulator for cold resistance[55].

It is a polymer mainly built of fructose units joined by a β (2→1) glycosidic bond and fructose or glucose units at the end. Due to its chemical structure fructose can be obtained after the hydrolysis of four different bonds: the terminal glucosyl to fructosyl, the terminal sucrosyl to fructosyl, internal fructosyl to fructosyl within the polymer chain, and the terminal fructosyl to fructosyl[56].

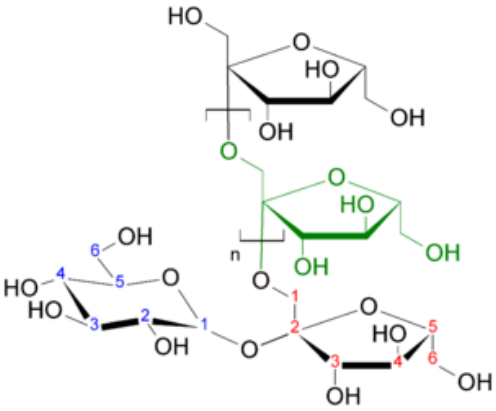

Figure 13: Inulin molecule

- Cellobiose and maltose

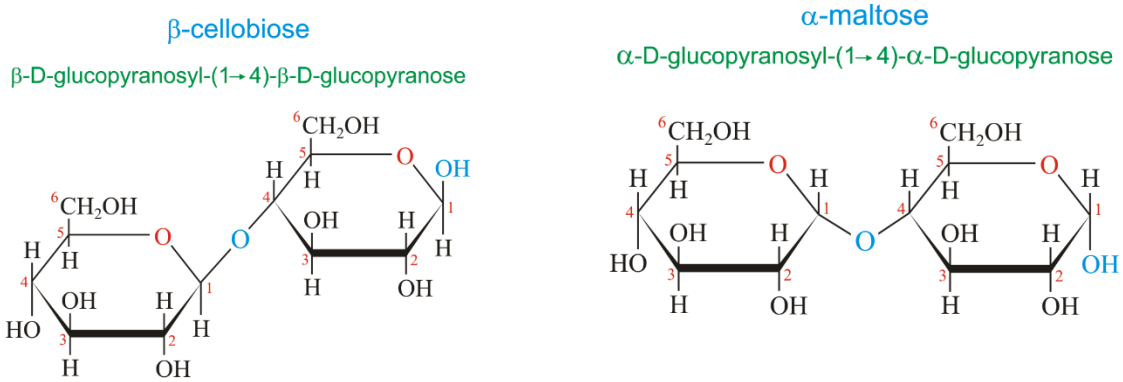

Figure 14: Cellobiose and Maltose

Cellobiose and maltose are reducing sugars consisting of glucose moieties linked by glycosidic bond. They represent two anomers: in cellobiose the glycosidic bond from the C1 is in the same plane of the CH_2OH substituent, giving a β-bond. Alternately, if the C1 and the substituent are in opposite planes, the α-bond occurs, yielding to maltose. Both of them can be hydrolyzed to glucose enzymatically or with acid.

1.2.2 From glucose to lactic acid

As mentioned before glucose can represent a valid alternative to the fossil feedstock as starting material for chemicals. Among the products that can be obtained the production of 2-hydroxypropionic acid, commonly known as lactic acid (LA) is of great interest.

As the scheme 2 shows, starting from this latter, it is possible to obtain a large variety of molecules, with a global market around 300-400 Kton per year [57].

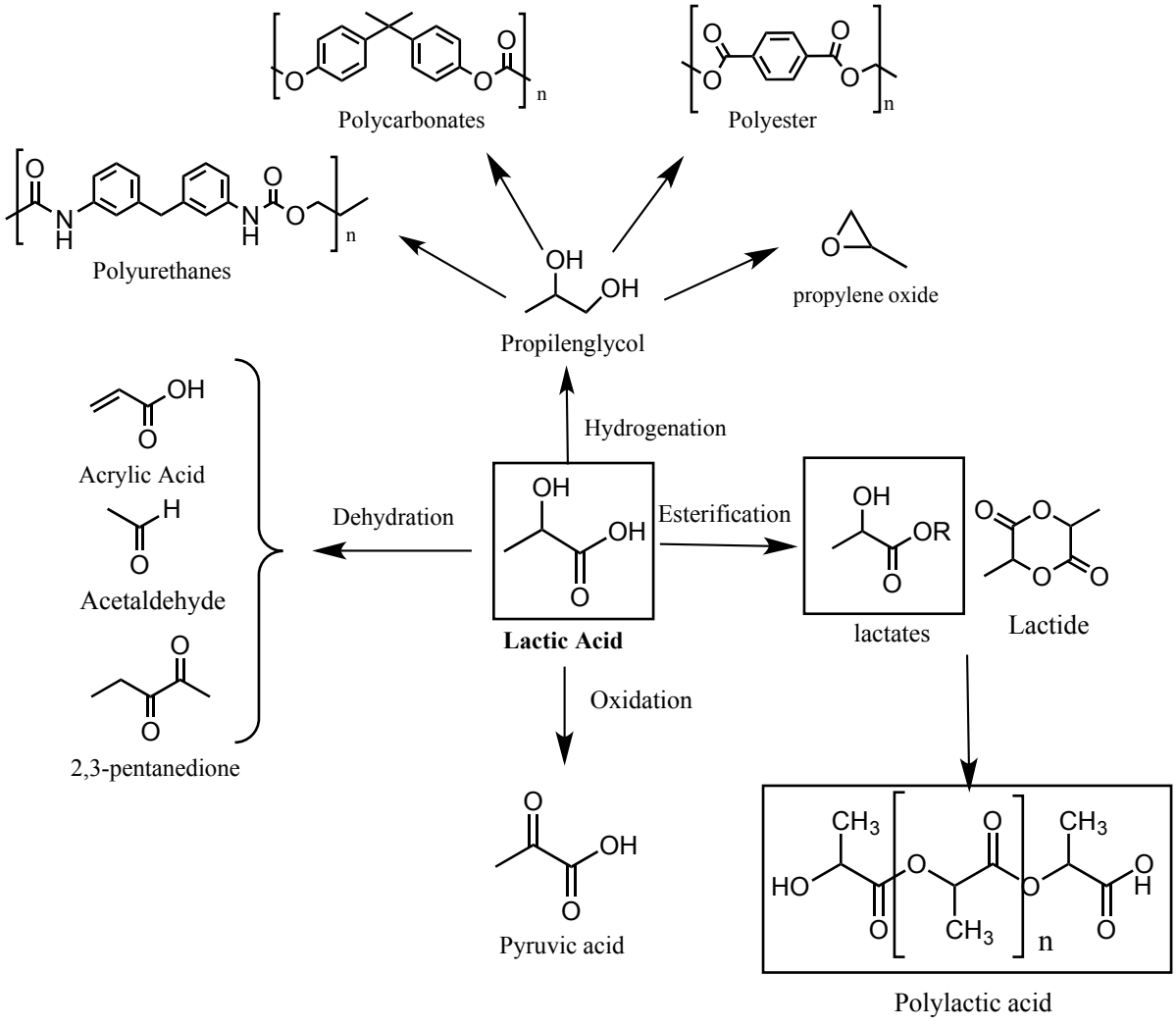

Scheme 2: Schematic representation of the chemicals and products that can be obtained from lactic acid.

Alternatively, LA is the building block of Poly-lactic acid (PLA), the first renewable and biodegradable bio-based plastic. Since 1990, the PLA production steadily increased, from 20 Ktons in 2002 [58] to 360 Ktons in 2013 [59], and it is expected to increase of the 10% annually until 2021[34].

Currently the main method for ML production involves fermentative formation of LA as first step, followed by lactide production [60](LD) and final ring opening polymerization, yielding the polymer (Scheme 3).

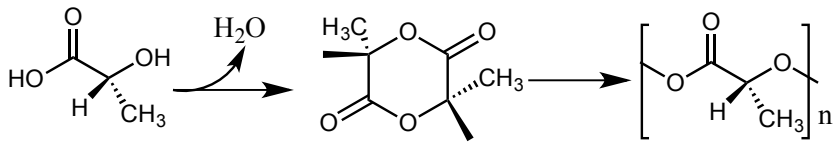

Lactic acid Lactide Polylactic acid

Scheme 3: Reaction pathway for the production of polylactic acid from lactic acid via lactide intermediate.

As already mentioned the employment of fermentative methods can limit drastically the productivity and price due to severe limitations that the technique requires.

Approximately one decade ago the catalytic conversion of carbohydrates started to emerge over the fermentative processes starting from trioses, hexoses or raw material as sucrose or cellulose.

1.2.3 Zeolites for biomasses conversion

The use of low-value and cheap sugars as starting substrates for the production of lactic acid involves cascade reactions catalyzed both by Brønsted and Lewis acids. In this case, zeolites with modified acidity are used, acting as multifunctional catalysts. Sn-Beta was initially found to selectively convert trioses to methyl lactate, even at low temperatures[61]. Starting from larger substrates, such as hexoses and pentoses, the catalyst was still capable to form methyl lactate even if with lower yields, since the increased complexity of the mechanism involves the formation of additional products. Moreover, the possibility of using different starting

material than glucose, alleviate the need to use a specific substrate that is one of the major limits for enzymatic processes.

From the raw starting material the reaction starts with the hydrolysis of the glycosidic bond (e.g sucrose or other polymers) producing the hexose glucose. In the presence of Lewis acidity, the isomerization of glucose to give the more reactive fructose occurs rapidly through an intramolecular 1,2-hydride shift, especially using Sn-zeolites[62,63].

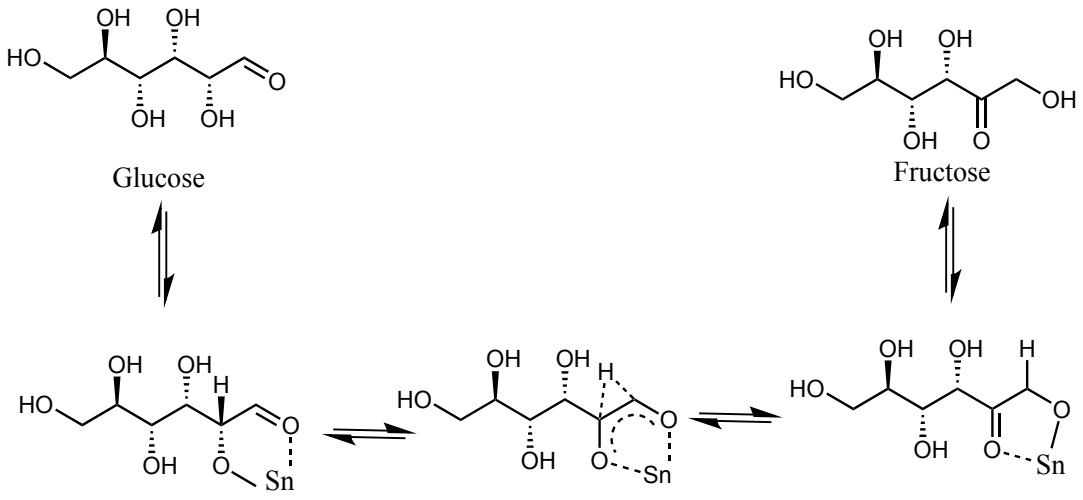

Scheme 4: Sn catalyzed isomerization of glucose into fructose.

By a retro-aldol reaction, fructose is splitted into the trioses glyceraldehyde (GLY) and dihydroxyacetone (DHA); after, a dehydration occurs leading to pyruvaldehyde (PAL) and instant acetale formation, according to the different solvent engaged. Finally a second 1-2 hydridee shift takes place, leading to the final alkyl-lactate (Scheme 5).

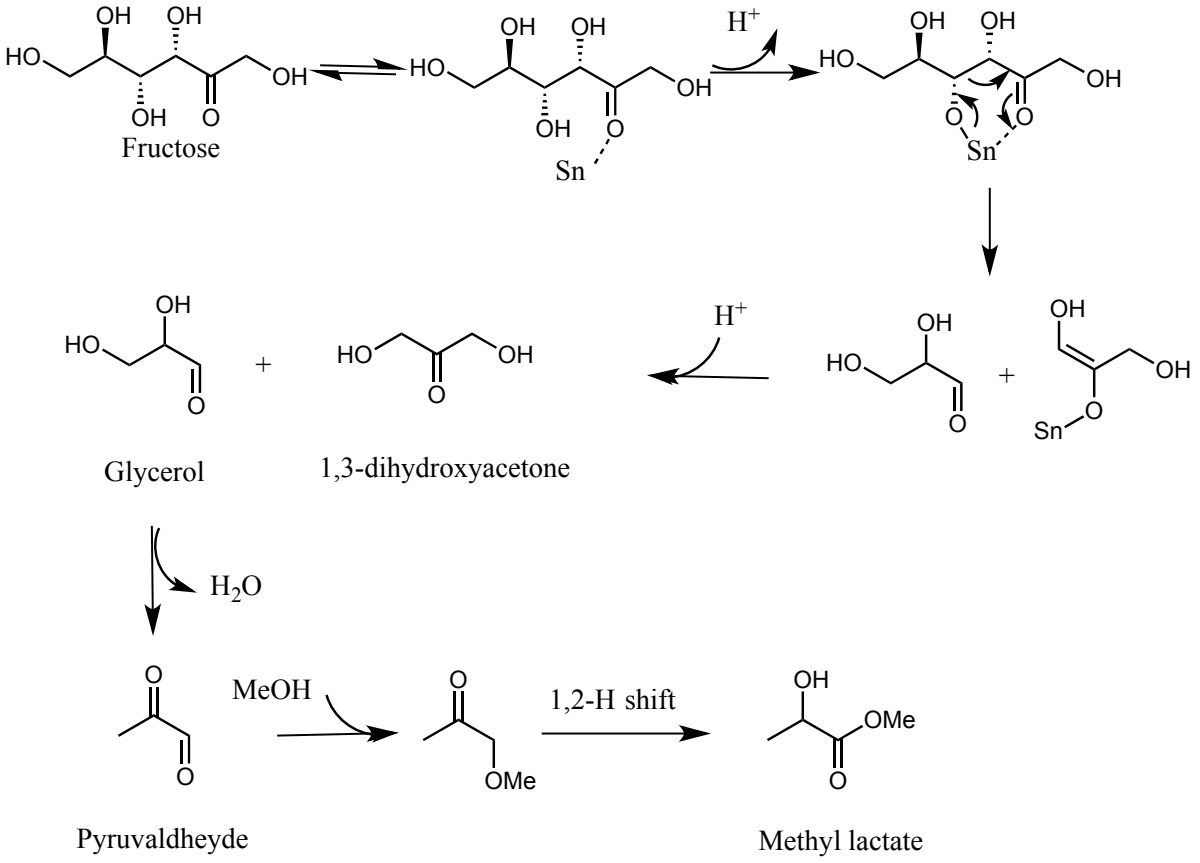

Scheme 5: Reaction pathway from fructose to methyl lactate in methanol with a Sn containing catalyst.

The analysis of the products mixture reveals the presence of traces of four-carbon α-hydroxy acid esters, not obtainable by classical fermentation. These include methyl vinyl glycolate (MVG), methyl-4-methoxy-2-hydroxybutanoate (MMHB) and trans-2,5,6-trihydroxy-3-hexenoic (THM). These molecules are chemically interesting due to the double and vinylic bonds: they can be functionalized and undergo polymerization, leading to new biomaterials.

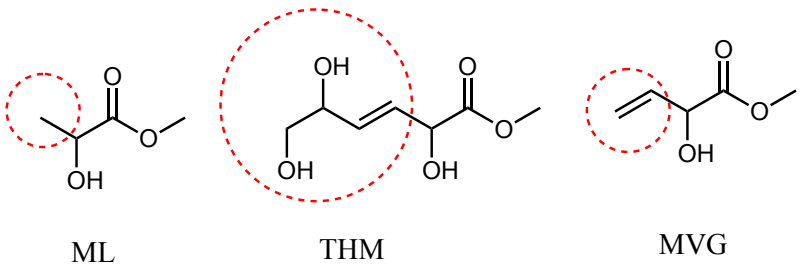

Figure 15: Representation of the functionalities of hydroxyesters which can undergo polymerisation

Mechanistically, the formation of MVG and MMHB from tetroses is similar to that of alkyl lactates, but their formation is associated with the reaction of glucose rather than fructose. The bond cleavage after the retro-aldol reaction leads to glycoladlehyde and tetrose sugars; from these latter, two cascade dehydratations take place giving vinyl glyoxal. The equivalent acetale is formed due to the use of an alchol as solvent, which after a 1,2-hydride shift gives MVG or MMHB.

The reaction pathway from glucose is illustrated in the scheme number 6.

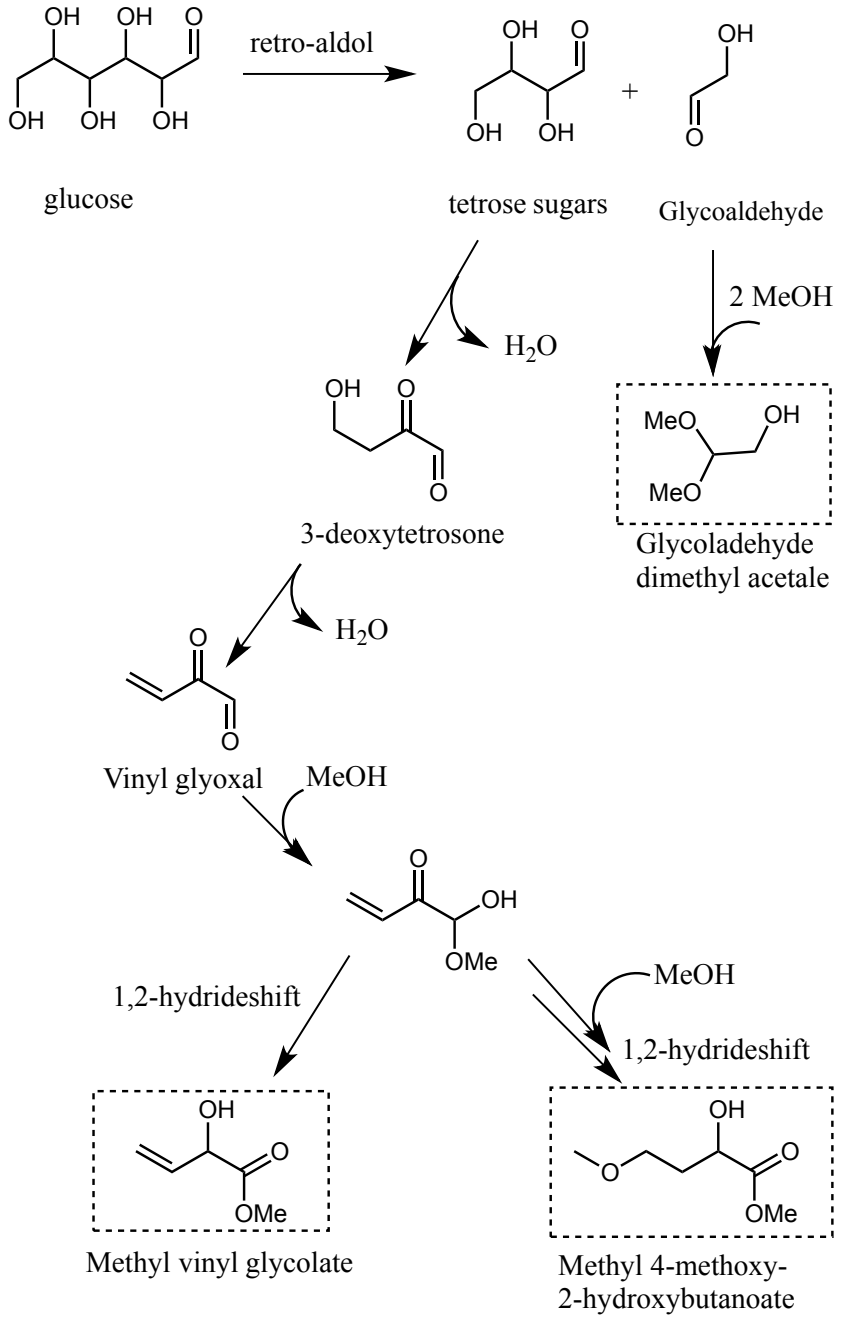

Scheme 6: Reaction scheme of the conversion of glucose into MVG and co-products.

The formation of THM is similar to the mechanism described in the previous scheme for MVG, with a first reaction with methanol on the aldehyde followed by a 1,2-hydride shift yielding the α-hydroxy ester.

The main by-products of this reaction are formed due to the presence of Brønsted acid sites and include: 5-hydroxymehtylfurfural (HMF), methyl glucosides and other furanic compounds.

In order to maximize the yield in alkyl lactate, some considerations must be taken into account:

- The choice of the solvent plays an important role: Holms et al. show that alcohols are preferred over water. Not only H_2O molecules act as competitors for the active sites but it leads to the amorphisation of the framework and degradation of Sn centers[42]. Water brings the formation of lactic acid but considering that it is a Brønsted acid, it will also lead the formation of unwanted HMF and levulinc acid[32]. Testing Sn-Beta using different alcohols as solvent, it has been revealed that methanol yields to the highest amount of methyl lactate, while changing to longer aliphatic chains (ethanol and propanol) a decrease in yield and substrate conversion is observed; [64]
- The balance between the Brønsted and Lewis acidity inside the zeolite plays a crucial role for the formation of methyl lactate. The isomerization from glucose to fructose occurs in the presence of Lewis acid sites, as well as the retroaldol cleavage to form ML. On the other hand Brønsted acidic sites promotes the formation of by products such as HMF, furfurals and methyl glycosides. Regarding these latter, they can be either methyl fructosides or glucosides. The first are kinetic products catalyzed from Lewis and Brønsted acid sites, therefore they are immediately formed as soon as the isomerization occurs. Since they are in equilibrium with fructose, it is possible to reconvert them in ML with longer reaction time and the right amount of Lewis acidic sites. The same does not happen for methyl glucosides, which represent by-products.

- Kinetic studies proved that the unmasking of methyl fructosides by hydrolysis is the RDS[65], hence a small amount of water aids the process without obstructing the catalysts stability[66].

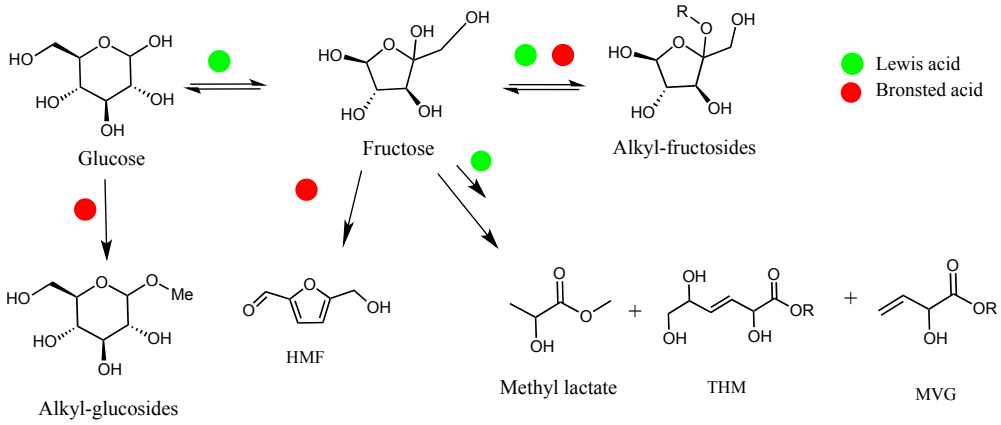

Scheme 7: Reaction involved for the formation of alkyl-glycosides, methyl lactate, HMF and other hydroxyesters

Tosi et al. investigate the influence of 0%, 2%, 5% and 10% of water in the reaction, proving its benefits over the rate of ML production, increasing the availability of free fructose during the first 20 minutes of the reaction. According to the previous discussion, bigger amount of water affect negatively the catalyst activity and stability.

- The presence of alkali in reaction media affects the Sn-beta catalysts performance and promotes production of methyl-lactate[67]. Even if the precise mechanism of the alkali on the catalyst is not clear yet, the cations are able to exchange the mobile protons in the zeolite framework and suppress a part of the Brønsted acidic behavior, limiting the side-reactions and increasing the selectivity to methyl lactate.

2. Aim of the project

The project of the thesis has been carried out in the group of Andres Riisager, at the Centre for Catalysis and Sustainable Chemistry, in the Technical University of Denmark (DTU).

The work has been performed under the supervision of the PhD Student Irene Tosi.

The objective of the research is the development of efficient catalysts for the production of methyl lactate and other hydroxyesters as polymers precursors, using different carbohydrates as starting material,.

In particular the work focused on investigating how the internal structure of a zeolite influences the products selectivity.

In the first part of the project different frameworks of commercial zeolites were tested using glucose as main substrate and subsequently for the conversion of different sugars.

At a later stage the attention have been pointed out to the formation of mesoporous systems instead of microporous, and how this type of alterations influences the activity and selectivity of the catalyst.

3. Materials and methods

This chapter includes the description of the methods involved for the synthesis and characterization of the catalysts in their structure and composition and the technique employed to quantify the amount of products obtained in the catalytic reactions.

Glucose (99,5%), sucrose (99,5 %), inulin, cellobiose (98%), maltose, nitric acid (>65%), $SnCl_4$ pentahydrate (98 %), tetraethylammoium hydroxide (TEAOH 35% water), cetyltrimethyl ammonium bromide (CTAB 98% wt), polydiallyldimethylammonium chloride (PDADMA 20 wt%), NH_4OH (50% w/w), methanol (99,8%, anhydrous), methanol-d_4 (99,8%), NaOH and dimethyl sulfoxide (DMSO >99,5%) were purchased from Sigma-Aldrich.

NH_4- Zeolites were obtained from Zeolyst International and calcined on a Nabetherm GmbH oven at 550 °C for 6 hours in order to obtain the H-form.

$NaAlO_2$ and fumed silica were acquired from Redel-de Haën and used without any further

treatment.

3.1 Synthesis of microporous catalysts with high Lewis acidity

In order to investigate the reactivity and selectivity when reacting with glucose, four different frameworks were selected: Beta, Faujasite, Mordenite and MFI.

BEA (19), USY (30), USY (6), MOR (6,5) and ZSM-5 (25) were used for the post-synthetic preparation of stannosilicate catalysts. The number in brackets represents the initial Si/Al ratio before the acidic treatment.

For the dealumination procedure all the frameworks were equally treated with 20 ml of HNO_3 13M per gram of zeolite, for 20 hours at 100°C in reflux conditions[18].

Subsequently, the zeolite was separated from the acidic solution by filtration, washed with distilled water until reaching neutral pH and dried overnight at 120°C.

In order to introduce Sn as active Lewis acid metal, $SnCl_4$* 5 H_2O was incorporated in the zeolite by the incipient wetness impregnation technique.

First, a blank test with only water was done on 0,5 g of zeolite, in order to detect the amount of solution necessary to fill-up the porosity. The precise amount of Sn precursor, calculated according to the desired Si/Sn ratio, was dissolved in water and subsequently added to the zeolite. The mixture was grinded manually to guarantee an optimal incorporation of the metal inside the framework.

The sample was firstly dried at 120 °C overnight and finally calcined at 550°C for 5 hours.

Microporous catalysts with enhanced Lewis acidity were therefore ready to be submitted to catalytic tests.

Framework type	**Si/Al ratio after dealumination**	**Si/Sn ratio**	**Cat.name**
BEA (19)	134	12,5	**Sn-BEA(12,5)**
		50	**Sn-BEA(50)**
		100	**Sn-BEA(100)**
USY(6)	15	25	**Sn-USY1 (25)**

		100	**Sn-USY1 (100)**
		200	**Sn-USY1 (200)**
USY(30)	70	25	**Sn-USY2 (25)**
		100	**Sn-USY2 (100)**
		200	**Sn-USY2 (200)**
MOR (6,5)	31	25	**Sn-MOR (25)**
		100	**Sn-MOR (100)**
		200	**Sn-MOR(200)**
ZSM-5	31	25	**Sn-ZSM(25)**
		100	**Sn-ZSM(100)**
		200	**Sn-ZSM(200)**

Table 2: Classification of the microporous Sn-zeolite synthesized; the first column reports the staring zeolite with the Si/Al reported in the brackets.

3.2 Synthesis of mesoporous catalysts

The mesoporosity inside the zeolite has been created following different pathways that are reported below.

3.2.1 Desilication

The desilication followed the procedure described by C.Hammond et al [68]**:** 30 mL of NaOH 0,2 M were added per gram of zeolite and stirred at 45 °C for 30 minutes, allowing the silicon extraction. Afterwards the zeolite was filtered, washed with distilled water until neutral pH was reached and dried at 100°C overnight.

Subsequent dealumination and Sn impregnation were performed on the desilicated zeolite, following the procedure mentioned above (chap. 3.2)

The mesoporous form of the BEA and USY frameworks with high Lewis acidity can be submitted to reactivity tests without any other treatment.

Framework type	Si/Al after desilication	Si/Al after dealumination	Si/Sn	Catalyst name
BEA (19)	14	127	100	**Sn-BEA(100) meso**
USY (30)	14	40	25	**Sn-USY (25) meso**

Table 3: Collection of mesoporous Sn-zeolite obtained by desilication and dealumination

3.2.2 Surfactant templating on a Sn-zeolites

According to the work done by Martinèz et al.[28], 1,75 g of cetyltrimethyl ammonium bromide (CTAB) were dissolved in 160 ml of NH_4OH 0,37 M. Afterwards, 2,5 g of Sn- zeolite were added and the mixture was stirred for 20 minutes before being transferred in a stainless steel autoclave.

The hydrothermal treatment was carried out for 10 hours at 150°C. The solid was filtered from the solution and washed with distilled water. After drying at 70°C, it was consequently calcined at 550°C for 5 hours in order to remove the template.

3.2.3 Surfactant templating on a H-zeolites

1,75 g of cetyltrimethyl ammonium bromide (CTAB) were dissolved in 160 ml of NH_4OH 0,37 M[28]. After, 2,5 g of H-USY with initial Si/Al ratio of 30 were added, and the mixture was stirred for 20 minutes before being transferred in a stainless steel autoclave.

After 10 hours of hydrothermal treatment at 150°C, the solid was filtered from the solution and washed with distilled water. The catalyst was dried at 70°C and consequently calcined at 550°C for 5 hours in order to remove the template.

The dealumination was performed following the previous method, adding 20 mL of HNO_3 13M per gram of zeolite and heating the mixture at 100°C under reflux for 20 hours. The solid was filtrated and washed with distilled water until neutral pH was reached. After drying overnight, Sn was insert by the wetness impregnation technique as described in chapter 3.2

3.2.4 Dissolution-Reassembly procedure

Following the work done by Martinez et al[28]., 1g of H-USY (30) was added to 63,6 mL of a 0,36M NH_4OH aqueous solution. The mixture was stirred for 2 hours and then 0.7 g of Cetyltrimethylammonium bromide (99%) (CTAB) were added. The solution was transferred in Teflon-lined stainless steel autoclave and a hydrothermal treatment was carried out for 48 hours at 150°C under static conditions. The autoclave was cooled down to room temperature; the solid was filtered off, washed thoroughly with distilled water and dried overnight at 70°C. In order to remove the template, the zeolite was finally calcined at 550°C for 5 hours.

The classical dealumination with HNO_3 (see chapter 3.2) was performed in order to create the vacant site, where Sn can be introduced through the incipient wetness technique with a Si/Sn equal to 25.

3.2.5 Hydrothermal synthesis with PDADMA

This synthesis follows the procedure reported by J. Zhang et al[35].: 0,424 g of $NaAlO_2$ and 1,59 g of NaOH were dissolved in 69 mL of water. 10,6 g of polydiallyldimethylammonium chloride (PDADMA 20 wt. %) were added and stirred until a homogenous solution was obtained. At this point 5 g of fumed silica were added and then stirred for another 12 hours. The mixture was allowed to crystallize into an autoclave for 96 hours at 180°C. After filtrating, washing with a large amount of water and drying at 80°C the zeolite was calcined at 550°C for 5 hours in order to remove the organic template.

3.2.6. Hydrothermal synthesis with PDADMA and TEAOH

A synthesis similar to the one reported in ch. 3.3.5 is employed with the surfactant PDADMA in addition to the TEAOH[69].

0,16 g of NaOH and 0.30g of $NaAlO_2$ were mixed with 32 mL of tetraethylammonium hydroxide (TEAOH, 25 wt.%). 4,8 g of fumed silica were added at the mixture and stirred manually to obtain a homogeneous solution. Subsequently 3 g of PDADMA (40 wt. %) were

included and mixed for 24 hours. The mixture was transferred into a stainless steel autoclave and a hydrothermal treatment was performed for 168 h at 140 °C.

3.3 Reactivity

3.3.1 Reaction conditions

All the reactions were performed in a Microwave reactor Biotage ® initiator +.

In a typical run 120 mg of substrate, 50 mg of catalyst, 5 mL of methanol and 80 µL of DMSO were added in a 5 mL vial. The reaction was performed for 2 hours at160 °C under autogenous pressure.

In order to improve the conversion of the substrate and the yield in methyl lactate, some alterations have been applied to the time of the reaction and to the loading amount of reagents (e.g same amount of catalysts and substrate).

Figure 16: Microwave 5mL vial

3.3.1.1 Microwave reactor

Microwave reactors take advantage of microwaves radiations efficiency of heating polar molecules or solution: these are forced to rotate with the field and lose energy in collisions.

Conventional heating usually involves the use of a furnace or oil bath: the heat is transferred from the wall to the bulk of the reactor by convention or conduction. The main disadvantage is that the core of the reaction takes longer to achieve the target temperature and hot spot might be generated, while, with an internal heating source, the process results more homogeneous. Even more microwave heating accelerates the rate of the reaction, the heating rate and lower the amount of energy employed.

Figure 17: Microwave reactor Biotage ® initiator +

3.3.2 Analysis of products mixtures

After the reaction, the products mixture was separated from the catalysts by simple filtration and submitted to NMR analysis.

A typical NMR tube was prepared with 500 µL of reaction mixture and 100µL of deuterated methanol (MeOD) as deuterium locking agent.

^{13}C NMR and HSQC were submitted on a Bruker Ascend™ 400 MHz and 800 MHz NMR for products quantification and unreacted sugars identification. A correction factor was calculated by the Senior Scientist Sebastian Meier in order to have a correlation between the instruments signal and the concentration of the analyte.

Figure 18: 800 MHz NMR

3.3.2.1 ^{13}C qNMR

Quantitative NMR was introduced more than 50 years ago, the first study was published in the pharmaceutical research field in 1963[70]. The main advantage of this technique is the possibility to correlate the peak area to the number of corresponding nuclei giving rise to the signal.

Therefore using an internal standard (e.g. DMSO), it is possible to quantify the amount of the molecule associated to a specific peak by comparison of the areas. The concentration of the analyte is calculated following the equation 1:

$$\text{Analyte concentration} = 2 \times \frac{\text{Integral Analyte}}{\text{Integral DMSO}} \times \text{DMSO concentration}$$

Equation 1: Formula used for the quantification of methyl lacatate and co-products after NMR analysis.

This method was employed for the quantification of methyl lactate, co-products (MVG, THM and glyceraldehyde) and by products (furfurals, HMF)[71].

3.3.2.2 ^{13}C-^{1}H HSQC

The Heteronuclear Single Quantum Correlation (also known as HSQC) is a NMR experiment first described by Geoffrey Bodenhausen and D.J. Ruben in 1980. The spectrum is given by the combination of a ^{1}H and a ^{13} C spectra, respectively in the X and Y axis of a graph resulting in a two dimensional spectra.

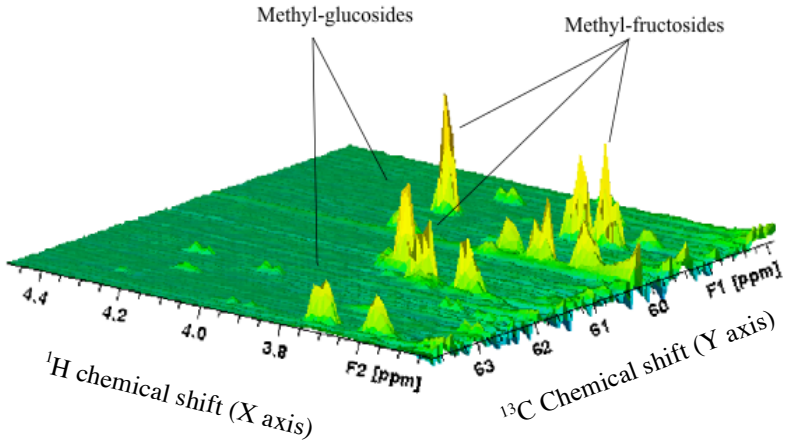

Figure 19: ^{1}H–^{13}C NMR spectral region of methyl-glycosides.

This method was applied for identification and quantification of all the different glycosides (Figure 16).

The ^{1}H–^{13}C HSQC spectra had a carrier offset of 63 ppm and a spectral width in the ^{13}C dimension of 22 ppm.

3.4 Catalysts characterization

This chapter includes the descriptions of the techniques employed for the characterization of the synthesized catalysts and the evaluation of their main properties (e.g. acidity, crystallinity, surface area etc.).

3.4.1 Composition properties: XRF

X-ray fluorescence is the secondary (or fluorescent) emission of X-ray from a material, when it has been previously excited by bombarding with high energy X or gamma (γ) rays. This

non-destructive technique allows to detect the chemical composition of a material, hence it finds wide range of applications in geochemistry, forensic science and archeology.

The phenomenon involved is the ionization of the atoms constituting the sample: X and γ-rays are energetic enough to expel inner electrons from the orbital in the atom, leaving a vacancy behind. As consequence, the atom configuration becomes unstable and external electrons start moving in order to fill the hole. In falling, a certain amount of energy related to differences between the two states is released from the atom as photon. The radiation emitted has a wavelength bigger that the incident one and is further detected separating the wavelengths of the radiation or sorting the energy of the photons.

Considering that each atom has electronic orbitals with characteristic energy, the amount of energy released can be directly associated with a specific element. Even more the intensity of each radiation emitted is directly related to the amount of element present in the sample.

The XRF PANalytical εpsilon3-XL has been used to investigate the amount of silicon, aluminum and tin present in every catalyst of interest, giving useful information regarding the acidity of the material and its ability to incorporate Sn.

The amount of residual Al and included Sn can be achieved applying to the value (express in Cps) a correction factor; this latter is obtained by the slope of a calibration line made with five samples with known amount of Al and Sn.

3.4.2. Structure properties

3.4.2.1 BET

This technique owns its name to its inventors – Brunauer, Emmett, Teller, who in 1938 published their article about the BET theory on the Journal of Chemical American Society.

The aim of this analysis is to measure the specific surface area of a material by the adsorption of a gas molecule on its solid surface. The employed gas must be chemically inert on the sample surface: N_2 is commonly employed to its boiling temperature (77K), but also water, argon and CO_2 can be considered.

The theory is an extension of the Langmuir concept: this latter assumes that each gas behaves as an ideal gas, and the adsorbate partial pressure is related to its volume adsorbed into the surface.

In the Langmuir theory each cavity can be occupied only by one molecule, hence only mono-layer adsorption is taken into account. The BET model considers also multi-layers of adsorbate gas but with some assumption:

- Gas molecules adsorb on a solid layer infinitely;
- Gas molecules only interact with adjacent layers;
- The Langmuir theory can be applied to each layer.

This technique finds wide range of uses in the catalysis field because it allows to detect the specific surface area (m^2/g) and the pores volume, which are fundamental properties of a catalyst.

It is important to take into account that the amount of N_2 adsorbed on the zeolite is influenced also by the amount of Al present in the framework due to its acidity leading to an overestimation of the measure. Even more, N_2 has a quadrupole moment which can interact with the electrostatic field created by the cation present in the zeolite[72].A more precise result can be obtained using Ar as adsorbate: being non-specific its adsorption is independent on the Al content and solely related to Van der Waals interactions with the surface.

According to the different size of the pore, a specific isotherm can be generated plotting the relative pressure of the adsorbate gas versus its volume. For microporous system a type I isotherm is observed, while type IV is reported for mesoporous (Figure 20). Regarding hierarchical zeolites, which have both features, a combination of the two isotherms is observed.

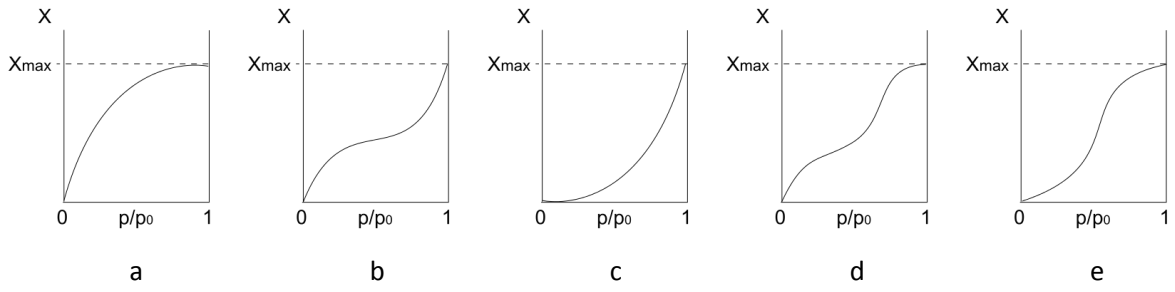

Figure 20: Adsorption Isotherms according to the BDDT classification: a) Type I; b) Type II, c) Type III, d) Type IV, e) Type V

Furthermore, plotting the pore width versus the derivative of the volume of adsorbate, it is possible to obtain a distribution graph where the average pore width of the zeolite is located in correspondence of the main peak.

The BET analyses have been employed to investigate the formation of mesopores using a Micrometrics ASAP 202 surface area and porosity analyzer.

3.4.2.2 XRD- X-Ray Diffraction

XRD is a rapid analytical technique, which can be employed for phase identification of a crystalline material, providing information on the structure and unit cell dimensions.

The method is based on constructive interference of monochromatic radiation and the crystalline sample: the radiations are generated and directed towards the sample.

When the Bragg's Law ($n\lambda = 2d \sin(\theta)$) is satisfied, the sample produce a constructive interference, creating a relation between the wavelength of the source and the crystal structure. The result is an unique fingerprint of the sample, which can be used to identify a particular structure of the zeolite. The XRD analysis were carried out with a Huber instrument, allowing the detection of the zeolite structure after the treatments.

3.4.3 Surface properties

3.4.3.1 TPD – Temperature Programmed Desorption.

This technique allows the detection of the number and strength of acidic sites for a given sample, involving desorption of a gas when the temperature is increased. Autochem II Chemisorption analyzer was employed to measure the acidity of the zeolites.

Figure 21 : Autochem II Chemisorption analyzer employed for the TPD measures.

NH_3 is the adsorbent gas, and the procedure requires different steps:

- Pre-treatment of the solid sample with helium at 500°C for 110 min in order to expel all the water molecules and impurities;
- Flow of 10% NH_3 in He at 150°C on the sample for 30 minutes, until the NH_3 saturates the sample

- Flow of He at 150 °C for 233 minutes in order to remove the physisorbed NH_3. This ensure a subsequent selective desorption of ammonia bonded to the sites by acid-base interactions;
- Heat of the sample up to 550°C with a heating rate of 10°C/min for 60 minutes and subsequent desorption of chemisorbed ammonia;

Recording the amount of ammonia desorbed by the sample and the temperature of desorption, it is possible to anticipate the amount and the strength of the acidic sites.

The Sn present in the framework makes weak (respect to Brønsted acid sites) bond with the ammonia, which is typically desorbed from these sites between 200 °C and 300°C. On the other hand, the Al acts as a Brønsted acidic center, and if it is still present inside the framework, the desorption of NH_3 is registered at higher temperature due to the formation of a strong bond.

3.5 Recovery test

One of the main advantages of the heterogeneous catalysis is the possibility to recycle the catalyst: its separation from the products mixture is as much important as its activity after the first cycle.

In order to test the stability of Sn-BEA(100) and Sn-USY(25), they were both submitted to recovery tests.

After performing a reaction in the conditions mentioned above (chapter 3.4.2), the catalyst was filtered with a Büchner filter, washed with MeOH and dried for 1 hour at 70°C. No further treatments were made on it before running a new catalytic test.

3.6 Catalytic tests with other substrates

In order to investigate the effect of mesopores on the conversion of dimers rather than the simple glucose, other substrates were taken into account.

Microporous forms of the selected catalysts were firstly tested to verify the possibility to convert the substrates. In case of positive results, also mesoporous catalysts were submitted to the same reaction and compared with the microporous systems.

The reaction conditions and procedure were kept constant (section 3.4.2) while the following

substrates were tested:

- Inulin;
- Sucrose;
- Cellobiose;
- Maltose;
- Starch.

4. Results and discussion

The aim of this work was the optimization of a heterogeneous catalytic system for the conversion of different carbohydrates into methyl lactate and other hydroxyesters.

In this chapter, the results obtained using different catalytic systems are discussed.

4.1 Characterization of catalytic systems

The table 4 resumes all the catalysts that have been synthesized. For microporous zeolites the characterizations have been done after the first screening reactivity tests, therefore in this table only the most active catalysts are reported. The complete list of all the microporous catalysts is reported on chapter 3.2. On the contrary, for mesoporous systems and hydrothermal synthesis, the succeeded of the synthesis was previously verified by XRD and BET.

	Synthesis method	Type of catalyst	Catalyst name
1.	De-alumination of H-BEA(19) and Sn-impregnation	Microporous	**Sn-BEA(100) micro**
2.	De-alumination of H-USY(30) and Sn-impregnation	Microporous	**Sn-USY(25) micro**
3.	De-silication, De-alumination of H-BEA(19) and Sn-impregnation (Ch. 3.3.1)	Mesoporous	**Sn-BEA(100) meso**
4.	De-silication, De-alumination of H-USY(25) and Sn-impregnation (Ch. 3.3.1)	Mesoporous	**Sn-USY(25) meso**
5.	Surfactant templating of Sn-BEA(100) (Ch. 3.3.2)	Mesoporous	**Sn-BEA(100) ST**
6.	Surfactant templating of Sn-USY(25) (Ch. 3.3.2)	Mesoporous	**Sn-USY(25) ST1**
7.	Surfactant templating of H-USY(30) (Ch. 3.3.3)	Mesoporous	**Sn-USY(25) ST2**
8.	Dissolution and reassembly of H-USY (Ch. 3.3.4)	Mesoporous	**Sn-USY(25) DR**
9.	Hydrothermal synthesis with PDADMA (Ch. 3.3.5)	Mesoporous	**BEA_HT1**
10.	Hydrothermal synthesis with PDADMA and TEAOH (Ch. 3.3.6)	Mesoporous	**BEA_HT2**

Table 4: Collection of all the synthesized catalytic systems.

4.1.1 Structure analysis- XRD

The XRD pattern for the zeolites reported in table 4 are shown below.

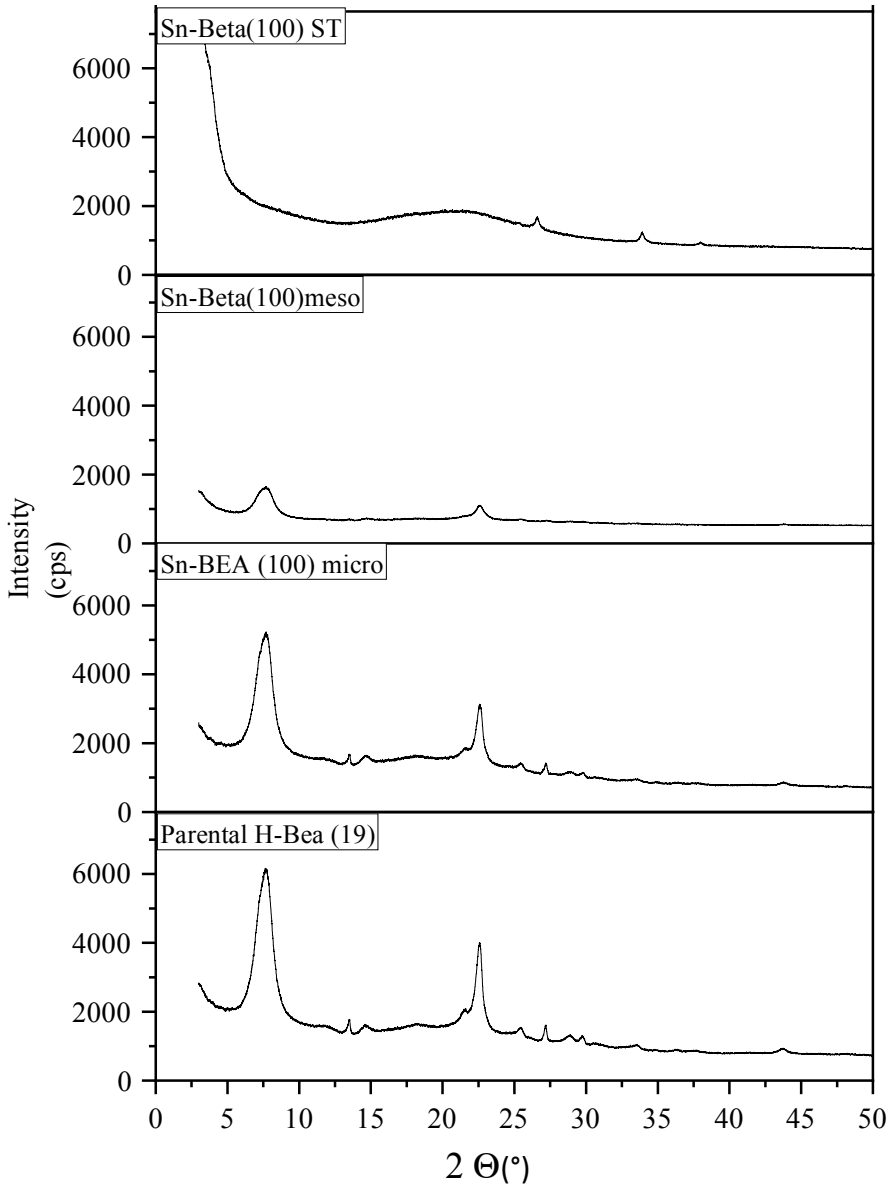

Figure 22: XRD diffractogran of different BEA framework. From the bottom: Commercial H-Beta, micriporous Sn-BEA(100) after dealumination, Mesoporous Sn-BEA(100) after desiication and dealumination, Mesoporous Sn-BEA(100) after surfactant templating treatment.

From the difractogram (Fig.22), it is noticeable how the dealumination (second spectra from the bottom) does not interfere with the typical structure of the BEA framework, reported at the bottom of the picture as comparison. The desilication causes a decrease in the crystallinity, but the two peaks around 8 and 22 degrees are still present, meaning that the structure is not completely lost. The decrease in intensity of the XRD peaks is due to a less efficient diffraction caused by the introduction of mesoporosity.

The XRD pattern evidences a successful incorporation of the Sn inside the framework and no evidence of the characteristic SnO_2 peaks (usually between 30 and 45 degrees).

The surfactant templating treatment of the Sn-BEA caused a partial destruction of the framework, and only a small peak around 25 degrees was still present; it is visible the presence of the two typical signals of the tin oxide specie. It can be hypothesized that during the treatment, the entrance of the surfactant has pushed out from the framework some of the Sn already present inside the structure, which is then deposited as inactive oxide.

The Figure 23 reports the XRD pattern of the hydrothermal synthesis with PDADMA of a Beta zeolite (ch. 3.3.5): it is evident the complete absence of a crystalline structure and only an amorphous phase was left. This implicates the absence of reactivity of the catalyst, as it has been proved from the catalytic test (ch. 4.4). The employment of TEAOH with the cationic polymer PDADMA was more successful, resulting in a crystalline beta structure as the figure 24 shows.

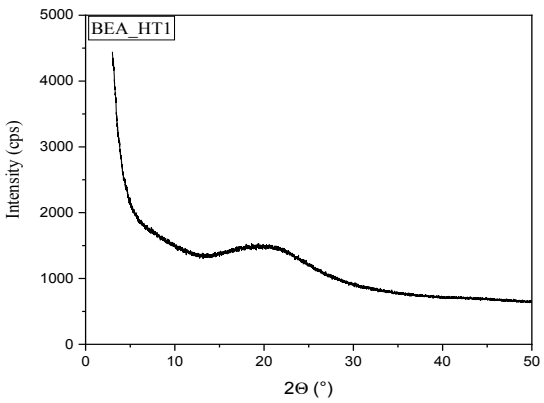

Figure 23: XRD pattern of zeolite after hydrothermal treatment with PDADMA (ch. 3.3.5)

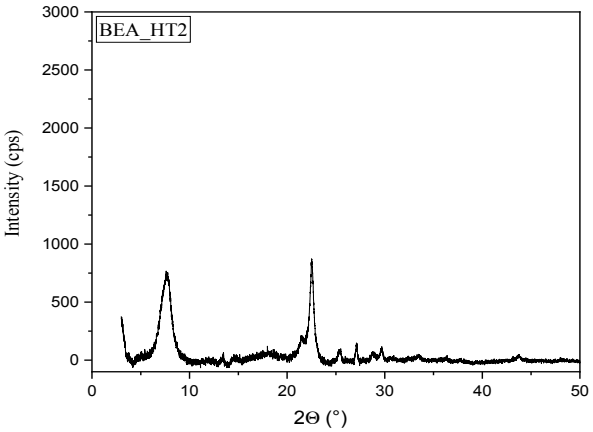

Figure 24: XRD pattern of the BEA zeolite obtained by hydrothermal treatment with PDADMA + TEAOH (ch.3.3.6)

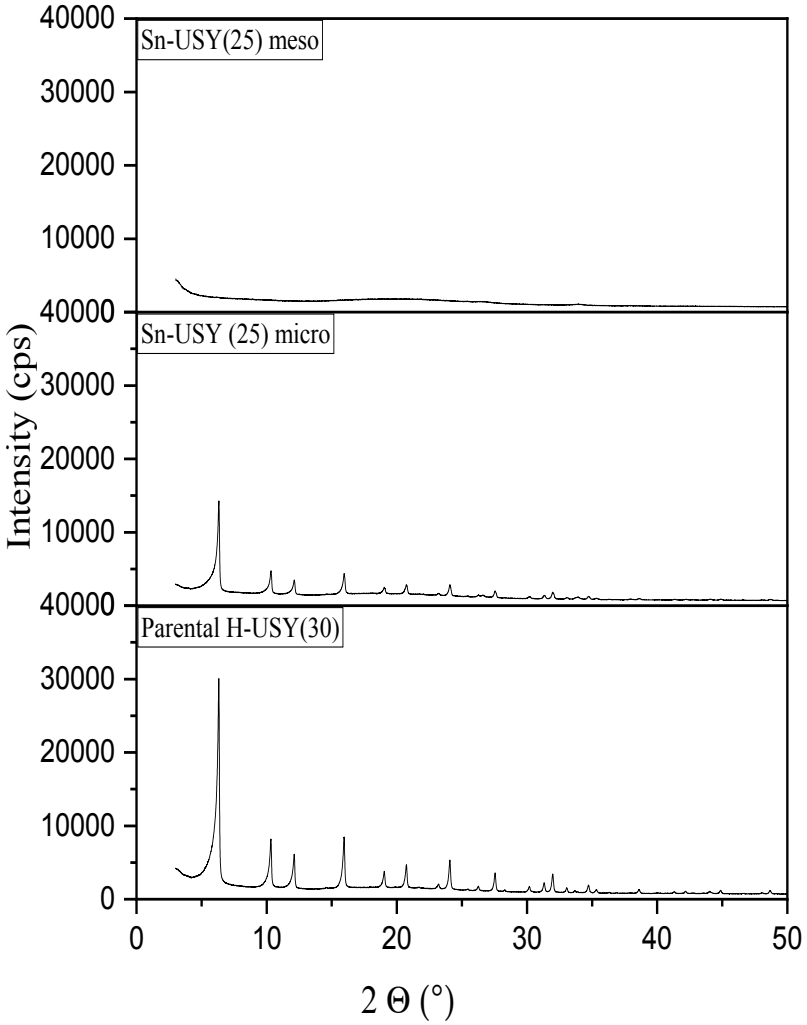

Figure 25: XRD pattern of different USY zeolite. From the bottom: commercial H-USY; Microporous Sn-USY (25) after dealumination; Mesoporous Sn-USY (25) after desilication and dealumination.

Analyzing the figure 25 it is possible to follow the behavior of the USY framework when it was submitted to different treatment. As for the BEA, the dealumination did not cause big changes to the framework: broader peaks were present due to the removal of Al, but the main crystal structure was maintained. On the contrary, the desilication caused a complete collapse of the structure; this was visible also during the treatment, since the zeolite was reduced in small particles and most of the starting material was dissolved.

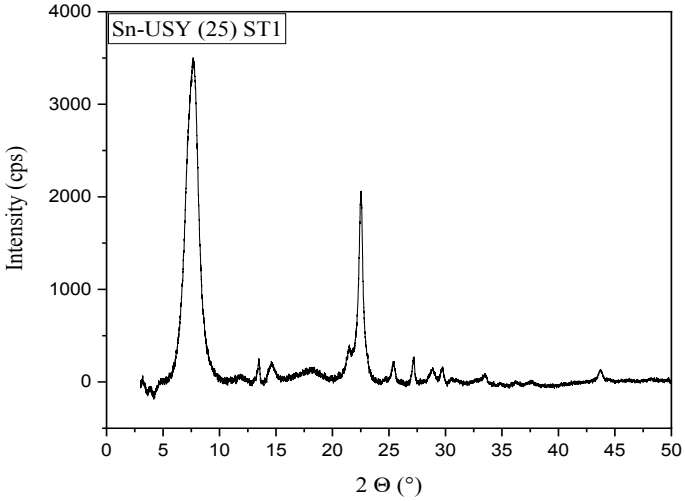

Figure 26: XRD pattern of the mesoporous Sn-USY(25)ST1 obtained by surfactant templating of a Sn-USY

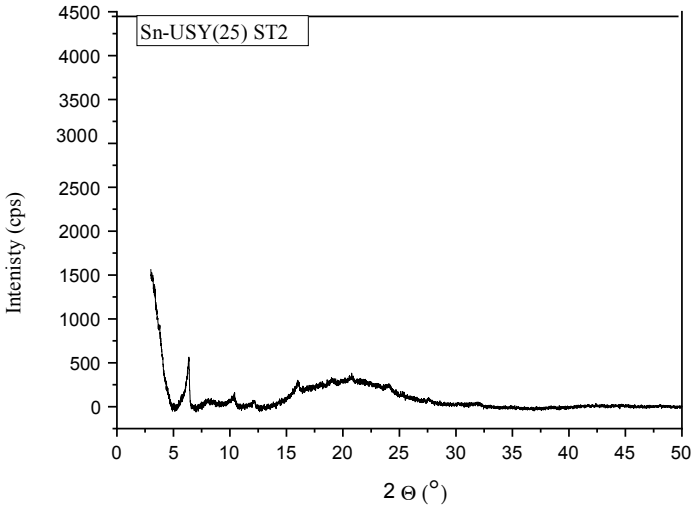

Figure 27: XRD pattern of the mesoporous Sn-USY(25)ST2 obtained by surfactant templating of a H-USY

In order to obtain at least one sample of mesoporous USY, two treatments with a surfactant template have been tried starting from both the Sn- and the H-USY (for the procedure see chapter 3.3.5 and 3.3.6). Figure 26 and 27 show the differences in the final XRD pattern, with a better result starting from the Sn-USY rather than the protonic form. Therefore, the first zeolite has been submitted to the full-BET characterization to verify the presence of mesopores and to subsequent catalytic tests.

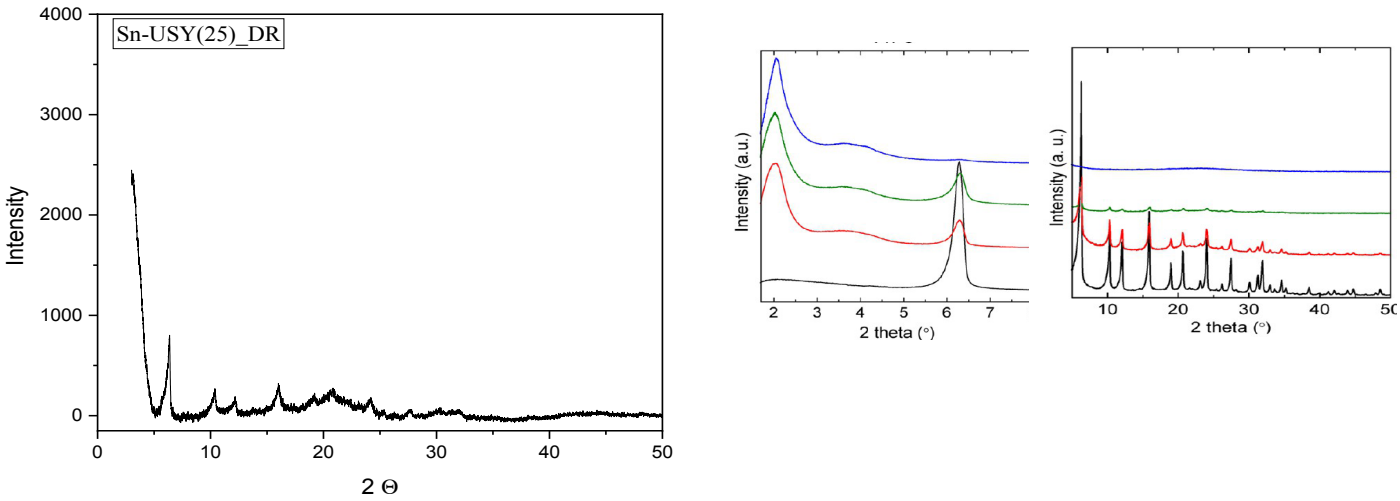

Figure 28: XRD pattern of the mesoporous Sn-USY(25) obtained by the dissolution-reassembly procedure. On the right side the XRD pattern obtained by Martinèz et al. is reported as reference

The spectra of the Sn-USY mesoporous (Figure 28) obtained following the dissolution and reassembly procedure was in accordance with the one obtained by Martinez et al. who tested successfully this method; since the dealumination showed no big impact on the zeolite framework, it was performed on the structure obtained for subsequent Sn impregnation. Before being submitted to catalytic tests, the presence of a mesopore structure was previously checked by BET analysis.

4.1.2 Acidity evaluation- XRF and TPD

The XRF analysis allows to investigate the amount of elements in the sample, to give an estimate of the acidity of the catalyst and the effectiveness of the dealumination procedure.

The value of the effective Si/Al and Si/Sn of the synthesized catalysts were obtained with the XRF analysis and reported in the Appendix (Table A1).

The evaluation of acidity can be reinforced by the TPD analysis: a desorbption of NH_3 is expected to happen between 200 °C and 300 °C due to the interaction with Lewis acids sites. A comparison between the microporous Sn-BEA(100) and Sn-USY(25) revealed an unexpected higher acidity for the first, despite the lower amount of tin (Figure 29). This can be a consequence of the presence of silanol gropus (Si-OH) left after the Sn-impregnation which act as weak Brønsted sites, and desorbed ammonia at temperature lower that 350 °C. However both samples show the typical NH_3 desorption curve with the increased Temperature.

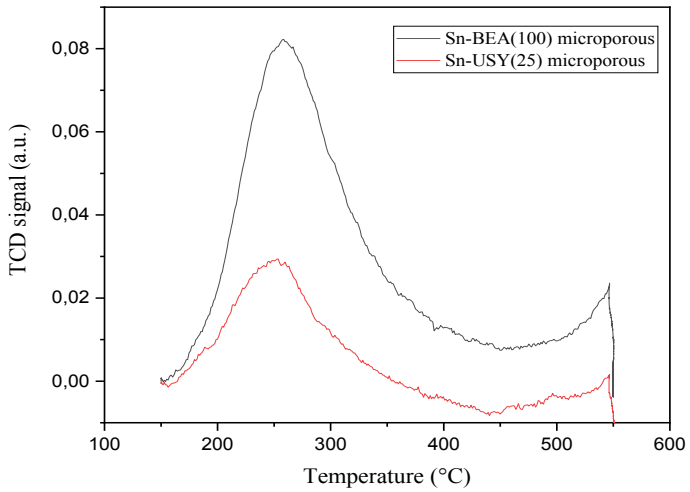

Figure 29: TPD NH3 desorption trend for microporous Sn-BEA(100) and Sn-USY(25).

4.1.3 Pore size analysis- BET

The BET surface area and pores size of the micro and mesoporous catalysts with better catalytic performances were analyzed by desorption of N_2 and Ar. Table 5 and 6 report a summary of the BET surface values, subsequently the characteristic adsorption isotherm are described.

Catalyst	BET surface area (m^2/g)	Average pore size (Å)
Commercial H-BEA(19)	609.7	21
Sn-BEA(100) micro	592.39	21
Sn-BEA(100) meso	637.7	48
Sn-BEA ST1	629.43	22
Sn-BEA(100) HT2	568	70

Table 5: BET values for the BEA framework

Catalyst	BET surface area (m^2/g)	Average pore size (Å)
Commercial H-USY(30)	803.75	24
Sn-USY(25) micro	757.6	25
Sn-USY(25) meso	370.1	--
Sn-USY ST1	539.72	26
Sn-USY (25) DR	626	34

Table 6: BET values for the USY framework

Analyzing the BET data of table 5, it is evident the success in obtaining a mesoporous system, due to the increase of the surface area. The same cannot be stated for the USY framework: in all the case there was a reduction of the surface area. In particular, the value for the desilicated

zeolite (entry 3 table 6) proves the collapse of the structure previously observed with the XRD spectra (figure 23).

Taking into account the XRD patterns and the BET values, the BEA framework showed the best behavior and an in-depth analysis of the micro and macropores have been carried out, with the aid of the Ar desorption technique.

The isotherm type I and type IV (Fig.30) obtained for the microporous and mesoporous zeolite, were in agreement with the literature data, confirming the success of the catalysts synthesis[61].

Plotting the pore size (Å) vs. dV of adsorbate, it was possible to obtain the pore volume of the two samples as the figure 30 shows:

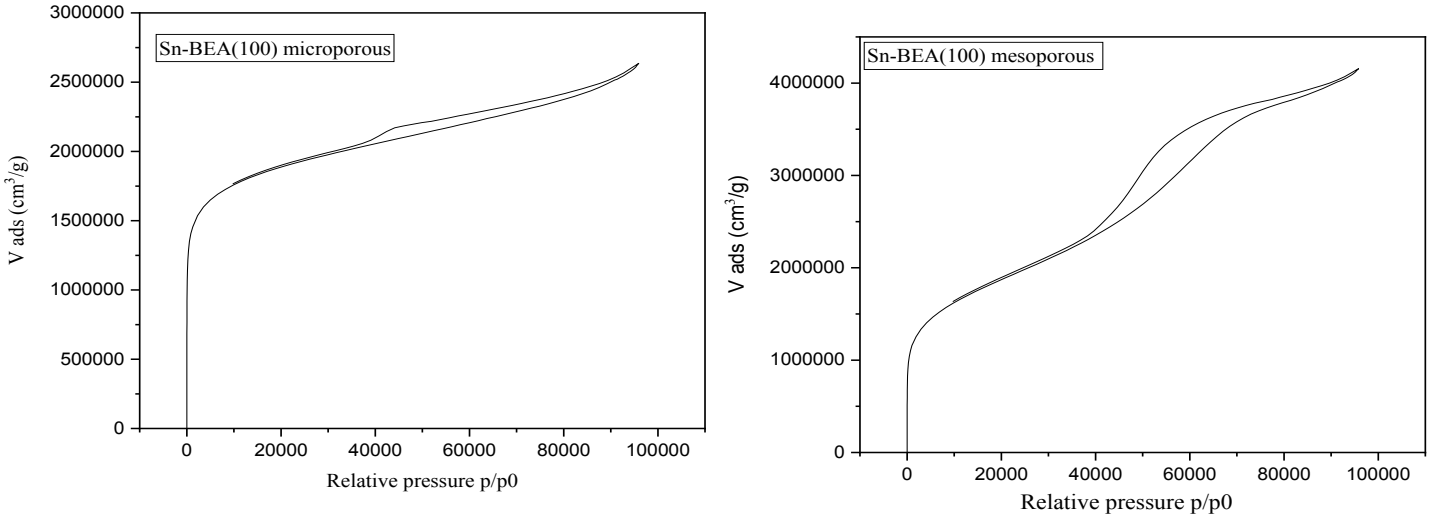

Figure 30: On the left is reported the isotherm type I for the microporous Sn-BEA(100); on the right the isotherm type IV for the mesoporous Sn-BEA(100) obtained with the desilication method.

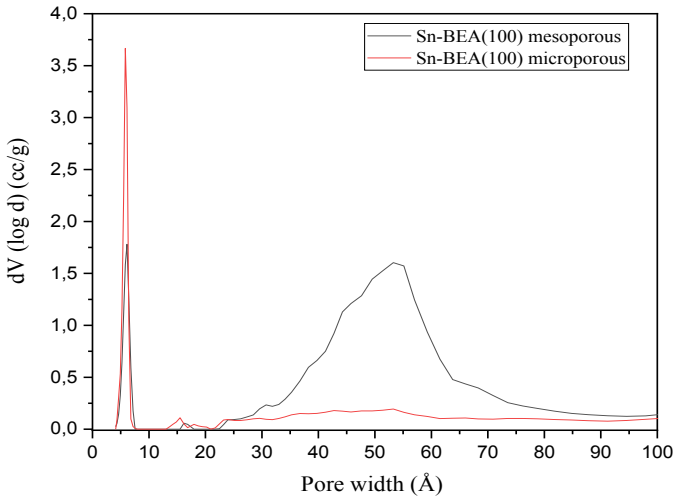

Figure 31: Pore size distribuition obtained plotting the pores width vs. dV. The first peak around 6 Å is meaning of the presence of micropores and it is evident in both samples. The second peak around 50 Å is present only for the mesoporous form of the Sn-BEA(100), confirming the success of the desilication procedure.

As it can be notice from the microporous zeolite, there is only a sharp peak around 7 Å, while the mesoporous plot presents a first peak at 6 Å and a second around 50 Å as prove that the formation of mesoporous by desilication was successful for the BEA sample.

4.2 Conversion of glucose using different microporous zeolite frameworks

From literature, it is well known that the BEA framework is suitable for the conversion of glucose into hydroxyesters when containing Lewis acidic centers such as Sn[43]. However, the detection of other frameworks useful for the conversion of sugars into different chemical compounds can lead to new interesting processes. Hence, after the synthesis, the above reported catalysts (ch. 3.2) have been tested for the conversion of glucose. The graphs below (Fig. 32 and 33) show the yields obtained regarding different products.

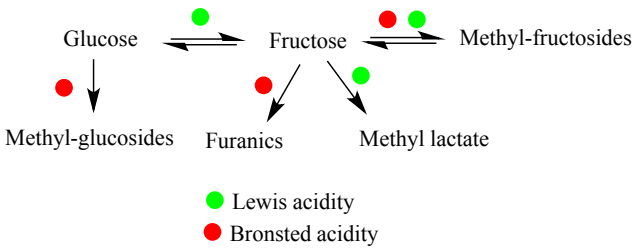

Scheme 8: Brief summary of the reaction pathway.

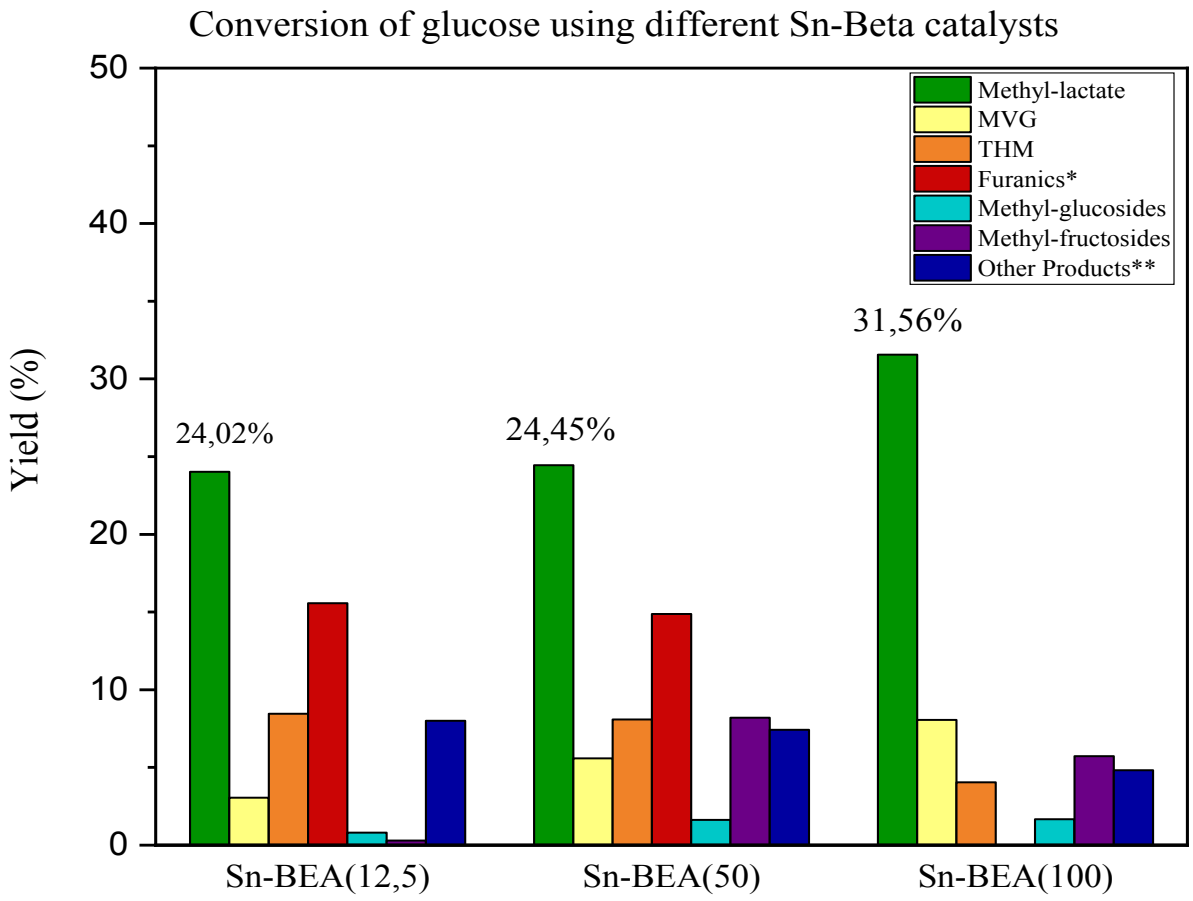

Figure 32: Yield (%) obtained for the different microporous Sn-BEA after dealumination and Sn impregnation. The number in bracket report the Si/Sn ratio.

Reaction conditions: 120mg substrate, 50 mg catalyst, 80 μ L DMSO, 5mL methanol, 160°C, 2 hours.

* Furanics percentage is obtained by the sum of the yields of 5-hydroxy methyl furfural (HMF) and furfural

** Other products include glucose, fructose, glyceraldehyde, 3-deoxy-γ-pentonolactone (DPL) and mannose

Among all the synthesized Sn-Beta, the most active toward methyl lactate is the one with lower amount of Sn (Si/Sn ratio 100). It is reported in literature[7] that, for the beta framework, there is a maximum amount of Tin that can be incorporated inside the cavities: higher amount can be deposited as SnO_2, hindering the active site for glucose transformations. Small amount of methyl glucosides (1.67 %) and no presence of furanics mean low Brønsted acidity and increased activity for the production of hydroxyl esters. Moderate amounts of THM (4.04%) and MVG (8.08%) are detected and, as stated before, these can represent interesting hydroxyesters for the formation of new bio-polymers.

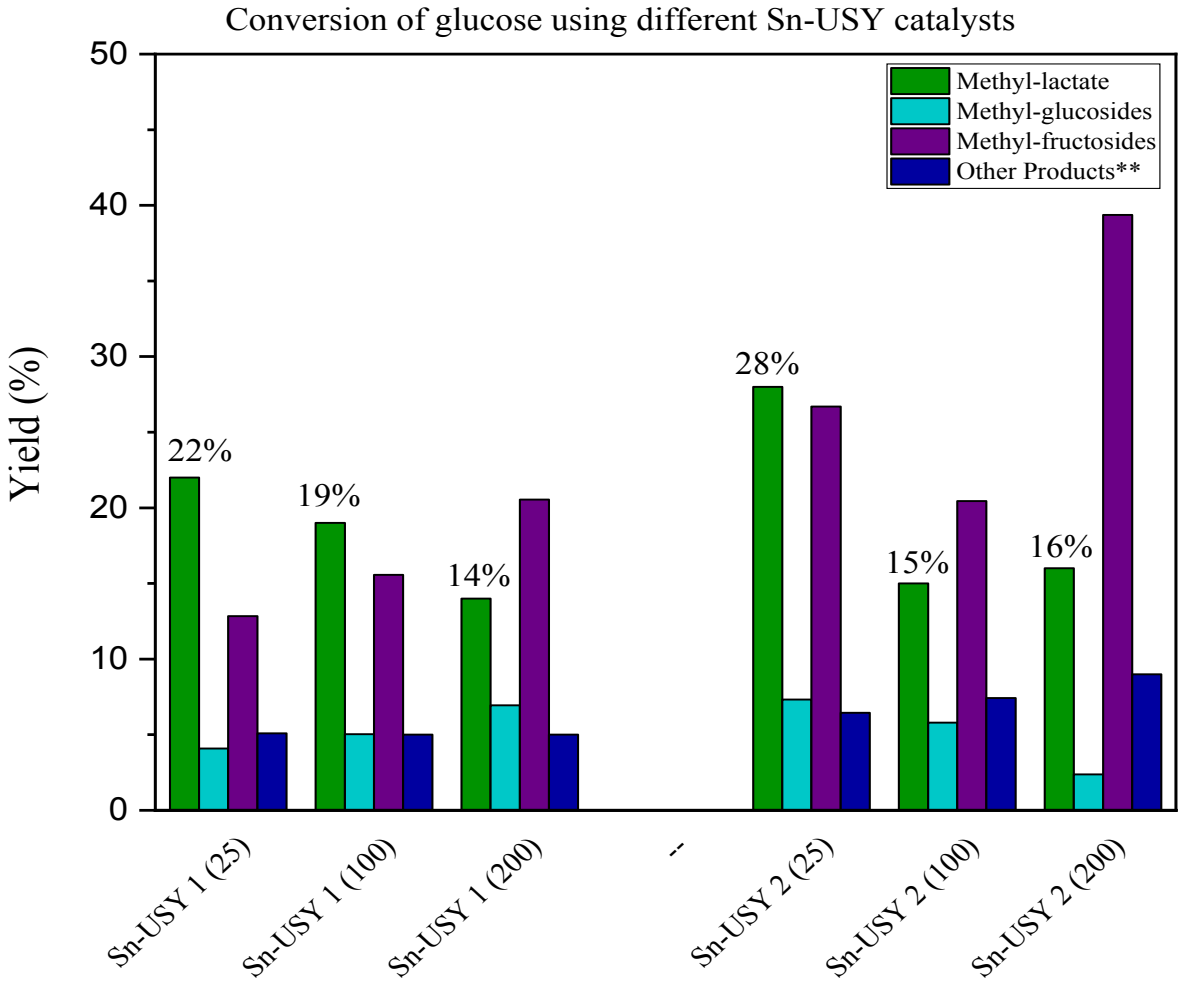

Figure 33: Yield(%) obtained for different microporous Sn-USY after dealumination and Sn impregnation. The number in brackets report the Si/Sn ratio. Reaction conditions: 120mg substrate, 50 mg catalyst, 80 μL DMSO, 5mL methanol, 160°C, 2 hours.

* Furanics percentage is obtained by the sum of the yields of 5-hydroxy methyl furfural (HMF) and furfural

** Other products include glucose, fructose, glyceraldehyde, 3-deoxy-γ-pentonolactone (DPL) and mannose

USY 1: USY with initial Si/Al = 6 USY 2: USY with initial Si/Al = 30

The results for the USY framework showed how the presence of Sn is crucial for the rapid formation of ML. Lowering its amount inside the framework led to major quantities of methyl-fructosides, as can be seen for the USY (200). It is true that these can be converted into methyl lactate but with longer reaction time. For that, the most active catalyst is the Sn-USY 2 (25).

The main difference between the BEA and USY frameworks was the different selectivity: MVG,THM and furanics were not found in any USY catalytic tests. Even if these were chemically interesting, their absence can potentially be translated in a greater yield towards methyl lactate.

In order to investigate different pores sizes, the same catalytic tests were performed using the Mordenite and ZSM-5 frameworks: results are reported in the graphs below (Figure 34). The zeolite Sn-MOR (25) showed no activity regarding methyl lactate or other hydroxyesters, and the same trend was observed for all the three catalytic systems (MOR (25), MOR (100) and MOR (200)). The high percentage of furanics and methyl glucosides induced to suppose that the concentration of Brønsted acid sites was considerably higher than those Lewis acidic.

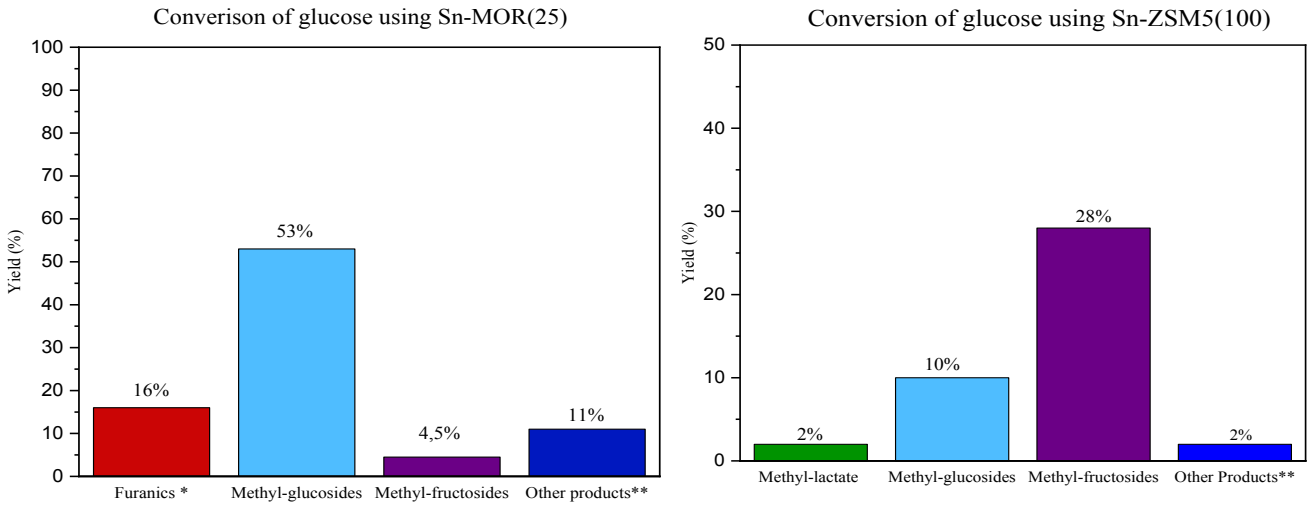

Figure 34: On the left is reported the percentage of the product obtained by glucose reaction with Sn-MOR(25). On the right the corresponding for the Sn-ZSM5(100). The number in brackets report the Si/Sn ratio.

Reaction conditions: 120mg substrate, 50 mg catalyst, 80 μ L DMSO, 5mL methanol, 160°C, 2 hours.

* Furanics percentage is obtained by the sum of the yields of 5-hydroxy methyl furfural (HMF) and furfural

** Other products include glucose, fructose, glyceraldehyde, 3-deoxy-γ-pentonolactone (DPL) and mannose

The XRF data reported in the appendix (Tab.A1) showed that a not efficient dealumination was conducted and the final Si/Al ratio is 31. However, the Si/Sn ratio, supposed to be 25, results in 6500 and explains the inactivity towards methyl lactate.

Catalytic tests with ZSM-5 did not lead to significant yield in ML: as the chart shows, the majority of products were methyl fructosides. The absence of HMF and furfural in the reactions can be attribute not to the low amount of Brønsted acid sites, but to the very small pores size of the catalysts: there is high probability that these by-products, together with humins, were formed but not able to pass through the channels out of the catalyst. Therefore, it was not possible to pick them out at the NMR but their formation is expected.

This first evaluation was done with the purpose of the selection of a restrict number of frameworks suitable for our reaction. Since Sn-BEA (100) and Sn-USY 2 (25) showed the best performance, they were synthesized in larger amount and submitted to further catalytic tests.

On the contrary, no further investigations were performed on Sn-USY 1, Sn-MOR and Sn-ZSM-5.

4.3 Recovery tests

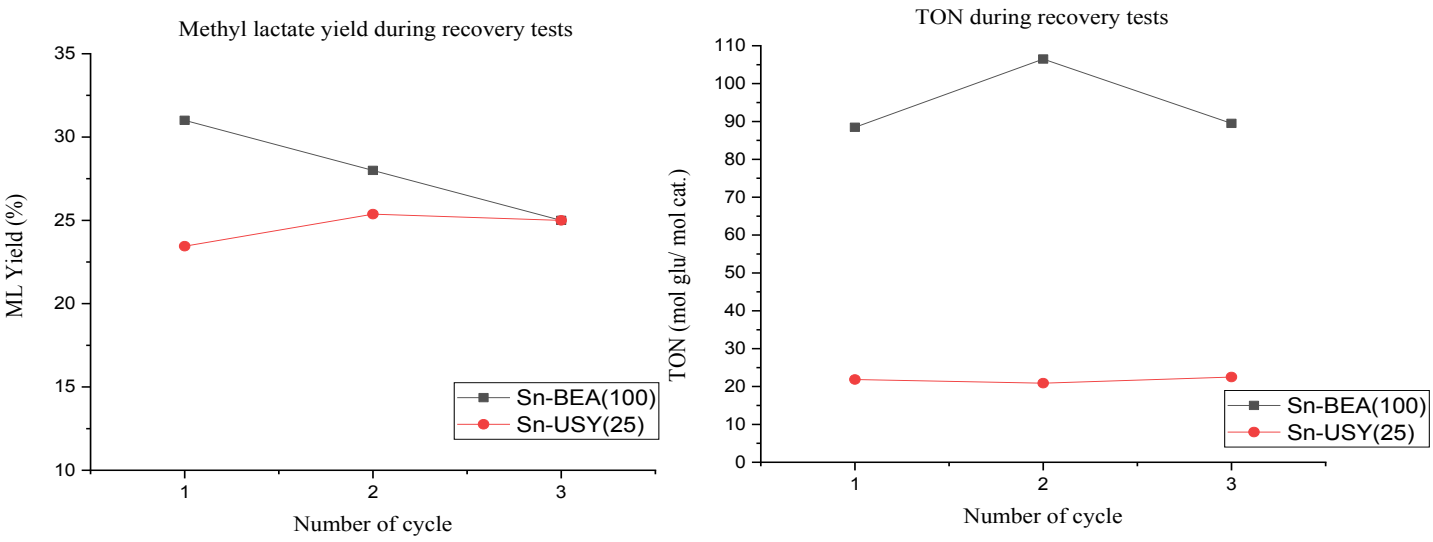

Figure 35: Yield in methyl lactate (on the left) and TON (on the right) during recovery test. The ratio between the substrate and the catalyst was kept constant according to the standard reaction conditions (120mg substrate;50 mg catalyst)

According to the results for the recovery tests (Figure 35) a slight decrease in the yield towards methyl lactate was reported for both catalysts of a small percentage, which made conclude that they were stable and easily reusable catalysts.

It is possible to assume that the Sn was well incorporated inside the zeolite framework and it did not leach into the solution: in that case, a deep reduction in ML would have been reported after the first cycle.

A better evaluation for the catalyst stability is the TON (Turnover Number), which can be calculated by the percentage ratio between the mol of unreacted substrate and the mol of catalyst (mol glucose /molSn).

The TON remained almost the same for both catalysts, confirming that the activity of both Sn-BEA (100) and Sn-USY 2 (25) was stable over the time.

4.4 Activity of mesoporous zeolites for the conversion of glucose

The mesoporous model for the Sn-BEA(100) and Sn-USY 2(25) were synthesized following the procedures listed in the chapter 3.3.

Even if their applicability interest is on bulkier substrates, their activity was formerly tested on glucose and results are reported in the graph below (Figure 36).

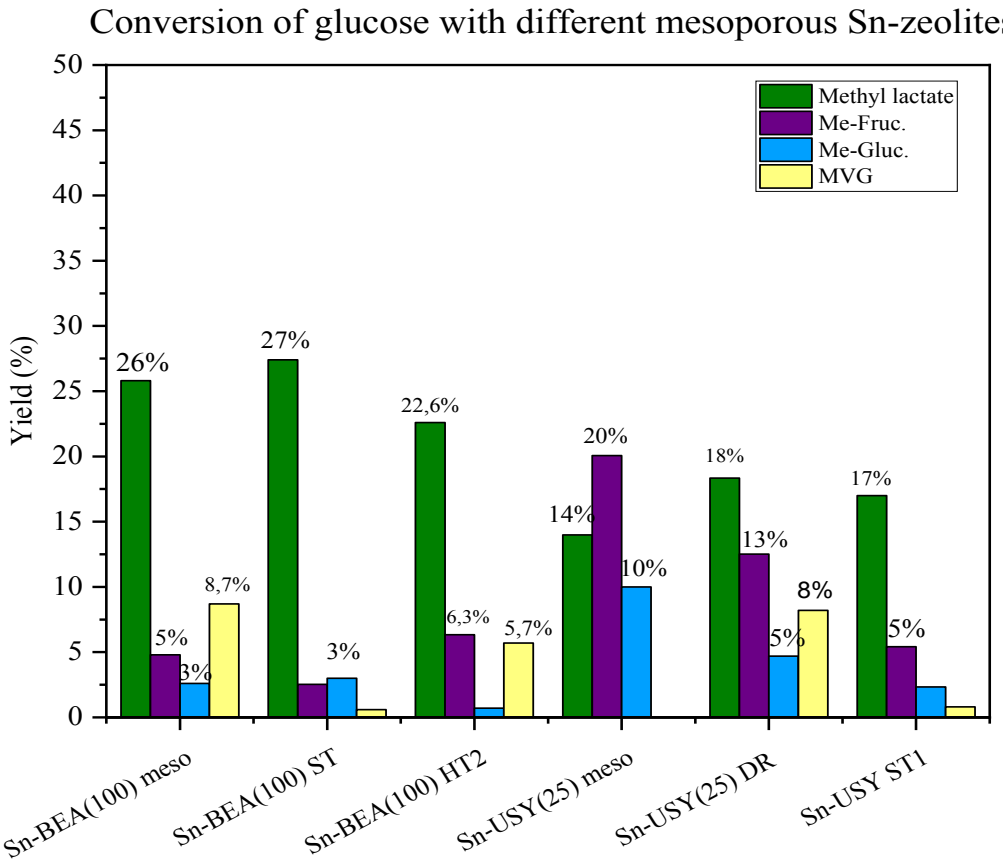

Figure 36: Methyl lactate (ML) and co-products percentage of different mesoporous catalyst when reacting with glucose. Reaction conditions: 120mg substrate, 50 mg catalyst, 80 μ L DMSO, 5mL methanol, 160°C, 2 hours.

Compared to the microporous systems, all catalysts show reduced activity in the reaction for the production of methyl lactate starting from glucose. In the case of the deslicated zeolite (histograms 1 and 4 Figure 36) the lower value can be attributed to the minor amount of Sn incorporated inside the framework, as the XRF reveals (see appendix Table A1), and to the reduced crystalline structure after the treatment (see XRD spectra ch.4.1.1).

In case of the surfactant template zeolite Sn-BEA(100) ST, Sn-USY ST1 and Sn-USY(25) DR a big amount of undetermined signals were revealed by the HSQC spectra; these can be attribute to the reduced crystallinity of the obtained zeolite: the catalysts were still active with the substrate but the reduced crystallinity compromises the selectivity towards methyl lactate and methyl-fructosides, causing the formation of unconverted intermediates, humins and furanic compounds.

Sn-BEA HT_1 did not reveal any activity nor towards methyl lactate or others compounds.

The XRD (see difractogram chapter 4.1.1 figure 23) reveals the absence of any crystallinity inside the framework. The XRF found in the appendix reports the presence of Sn but we can suppose that all the Sn introduced was present as inactive oxide species. Therefore no further experiments have been carried out with this catalyst. Better results were achieved with the hydrothermal synthesis with both PDADMA and TEAOH, with positive results both in activity and selectivity towards ML.

4.5 Activity of the catalytic systems for the conversion of bulky substrates

4.5.1 Catalytic tests on inulin

Inulin was investigated as bulky substrate due to its structure made up of fructose and glucose units; first, with microporous catalysts (Figure 37) and later, with the mesoporous catalysts that have been selected after the reactions on glucose (table 7).

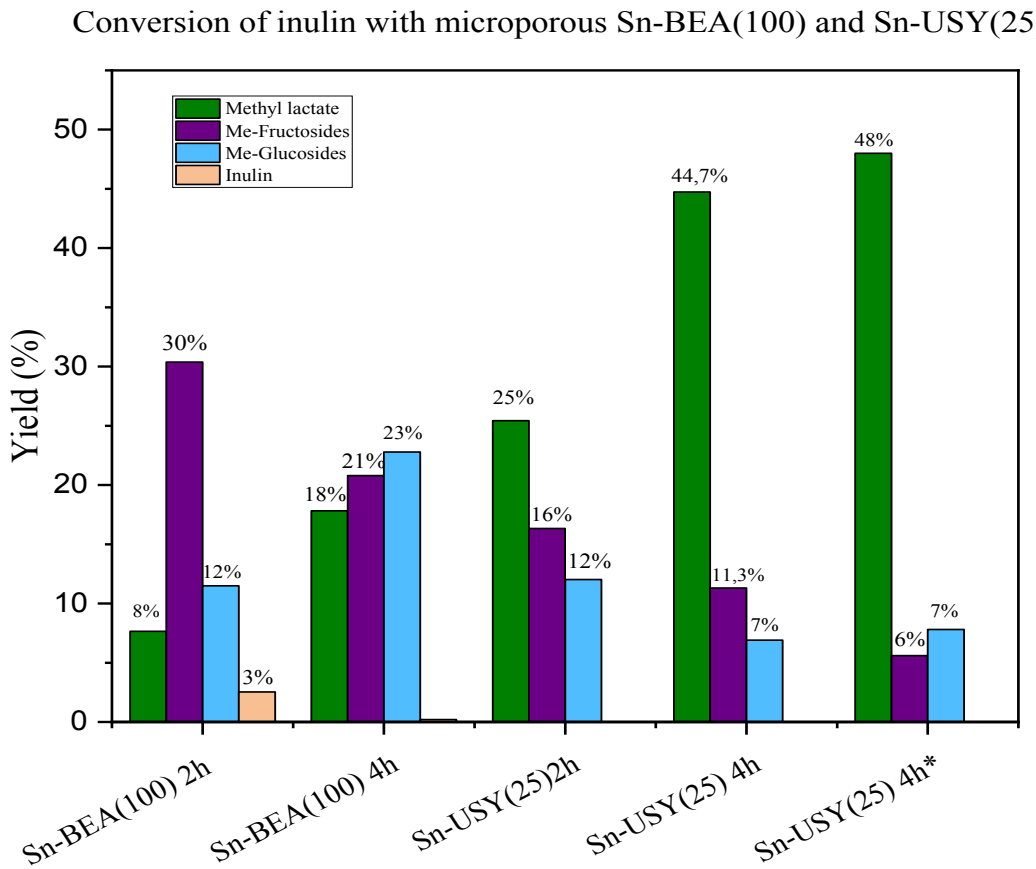

Figure 37: Methyl lactate and co-products percentage of micriporous Sn-BEA(100) and Sn-USY(25) when reacting with inulin. Reaction conditions: 120mg substrate, 50 mg catalyst, 80 μL DMSO, 5mL methanol, 160°C.

*= 4 hours with 10% H_2O.

From the results, it is possible to observe that the two catalysts were both active in the transformation of inulin and no relevant formation of MVG, THM and furfurals occured. The Sn-USY(25) was capable to convert much more substrate than the Sn-BEA(100). The hydrolysis of inulin was slower with the BEA rather than the USY: in fact, the USY, besides the intrinsic high Brønsted acidity, presented more Sn as Lewis acid active metal which was capable to hydrolyze the glucosydic bond of the starting material. After 2 hours all the substrate was hydrolyzed, while a little amount (2%) was still present with the BEA.

In order to accelerate the hydrolysis of inulin, 10 % of water was added to the reaction: the presence of 10 % of water speeded up the hydrolysis of the oligomer , influencing positively the whole reaction pathway, with a final increase of methyl lactate percentage.

Since inulin showed promising results, the selected mesoporous systems were tested for its conversion (table 7).

INULIN	ML	Me-Fru	Me-Glu
Sn-BEA(100) meso	8,75 %	41,70 %	4, 78%
Sn-USY(25) meso	12,07 %	15,47%	15,37%
Sn-BEA(100) ST	19.52%	9.24%	1.31%
Sn-USY(25) DR	19.7%	29.9%	3.35%
Sn-BEA HT2	9,88%	57,7%	3,82%

Table 7: Methyl lactate and co-products percentage of different mesoporous Sn-zeolite when reacting with inulin.

Reaction conditions: 120mg substrate, 50 mg catalyst, 80 μ L DMSO, 5mL methanol, 160°C, 2 hours.

Surprisingly, among Sn-BEA(100) and Sn-USY(25) de-silicated and de-aluminated, only the BEA behaved as expected (table 7 entry 1): since inulin is a bulky substrate, the presence of mesopores should facilitate the accessibility to the active sites, with subsequent increased yields compared to the microporous catalyst. The BEA showed a slight increase in ML and

Me-fructosides formation (1% and 10% more respectively), while the opposite trend was observed for the USY.

From the XRD (chapter 4.1.1 figure 25) is evident how the desilication caused a collapse of the Y structure with consequent partial loss of crystallinity: this catalytic system was therefore not entirely reliable for investigating shape selectivity effects of mesoporous systems.

The Sn-BEA(100) ST1 (table 7, entry 3) yielded to higher percentage of methyl lactate, but low amount of methyl fructosides and high percentage of carbon loss. The HSQC spectra showed a big amount of unidentified peaks, which might be assigned to intermediate and furanics that are formed because of the partial loss of crystallinity. Hence this catalyst was still active and the high surface area allowed the access of inulin to the active site, but due to the poor crystallinity framework left, the selectivity was declined drastically.

The mesoporous Sn-USY(25) DR (table 7, entry 4) showed activity regarding inulin but probably due to a decrease in crystallinity the yield in methyl lactate was lower than its microporous form. From the HSQC spectra many undefined peaks were visible and can be assigned to by-products formation prompted by lack of a crystalline structure.

4.5.1.1 Initial rate experiments

In order to better understand the reactivity of inulin inside the mesoporous system, reaction at short time (1.30, 10 and 15 minutes) were performed (Figure 38).

Analyzing the HSQC spectra, it was possible to investigate the rate of the inulin hydrolysis and the immediate formation of methyl fructosides, allowing the study of the substrate diffusion into the porosity. These studies were carried out with the Sn-BEA(100) microporous and mesoporous obtained by desilication and hydrothermal treatment wuth PDADMA and TEAOH, which showed positive results, both in terms of activity and retained crystallinity.

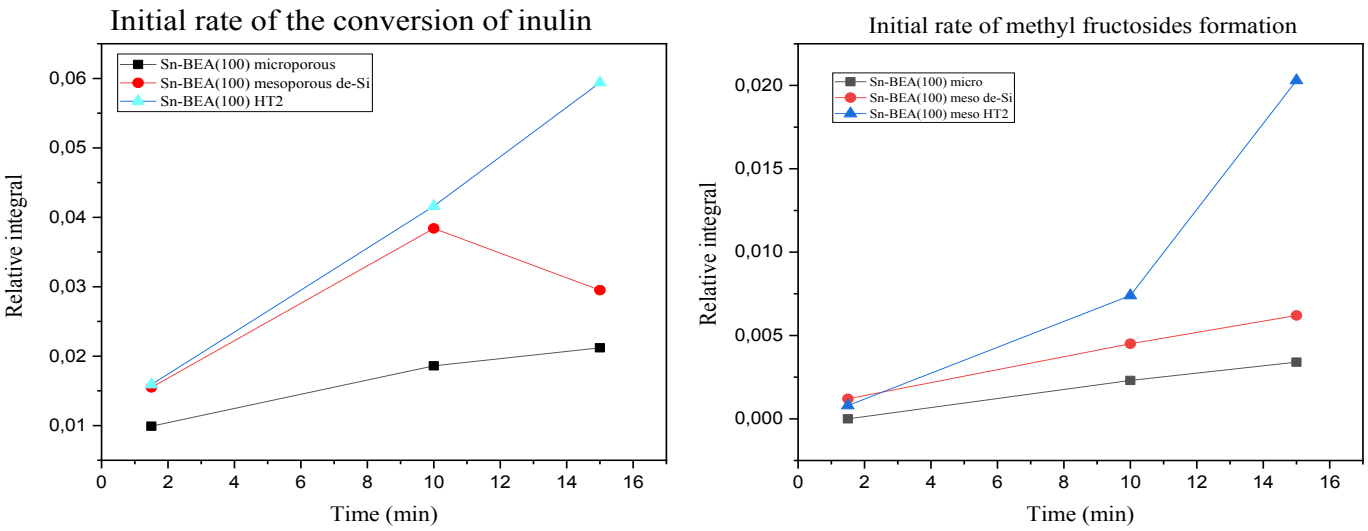

Figure 38: Trend of inulin conversion (left) and methyl- fructosides formation (right) of microporous and mesoporous Sn-BEA(100). Reaction were carried out at 1,50, 10 and 15 minutes, with 120mg of substrate, 50 mg catalyst, 80 µL DMSO and 5 mL MeOH at 160°C.

Inulin was dissolved in MeOH in acidic conditions and with the use of catalysts. The low intensity of the signal at very short times was due to an incomplete dissolution; for the mesoporous system the complete dissolution occured after 10 minutes and then the signal decreased accompanied by the formation of methyl fructosides. From the graph above, it is evident that the mesopores aid the entrance of the substrate into the zeolite channels accelerating the dissolution of the substrate.

For the microporous system, the low intensity of the inulin peak means the incomplete dissolution after 15 minutes.

As expected, after 1.30 minutes methyl fructosides were absent in the microporous system, while a small amount was reported for the mesoporous: in addition to the accelerated dissolution of inulin, the more accessible sites encouraged the formation of bulky molecules. The steeper slope observed for the mesoporous system proved that the methyl fructosides formation occured more rapidly than the one detected in the microporous, speeding up the reaction rate.

4.5.2 Catalytic tests on sucrose

Sucrose is one of the most abundant simple sugars, made of glucose and fructose units. Therefore, it has been chosen as substrate to perform a series of catalytic tests, first with microporous Sn-BEA(100) and Sn-USY(25) (Table 8) and subsequently with the mesoporous form (Figure 39).

SUCROSE	ML	Me-Fructosides	Me-Glucosides	MVG	THM	Furanics
Sn-BEA (100) micro	19.67 %	30.37 %	11.50%	3.24%	5.82 %	12 %
Sn-USY (25) micro	25.00 %	15.50 %	4.13 %	8.10%	8.13%	9.59%

Table 8: Methyl lactate and co-products percentage of different microporous Sn-zeolite when reacting with sucrose.

Reaction conditions: 120mg substrate, 50 mg catalyst, 80 µL DMSO, 5mL methanol, 160°C, 2 hours.

The presence of Brønsted acid sites allowed the fast solvolysis of sucrose into glucose and methyl fructosieds that can be further hydrolyzed into fructose and then transformed into methyl lactate. On the other hand, glucose can also isomerize into fructose in the presence of Lewis acid sites and produce methyl lactate.

Therefore, they represent the majority of products, as can be seen for the Sn-BEA.

In accordance with Holm et al.[58] considerable amount of MVG and THM were reported, since their formation follows a similar reaction pathway to the production of methyl lactate. These hydroxyesters were previously observed in the reactions with the BEA framework but not with the USY (chapter 4.2).

As for inulin, since sucrose gave positive results, the same catalytic tests have been conducted with the two top-down mesoporous forms. Results are reported in the graph below (figure 39).

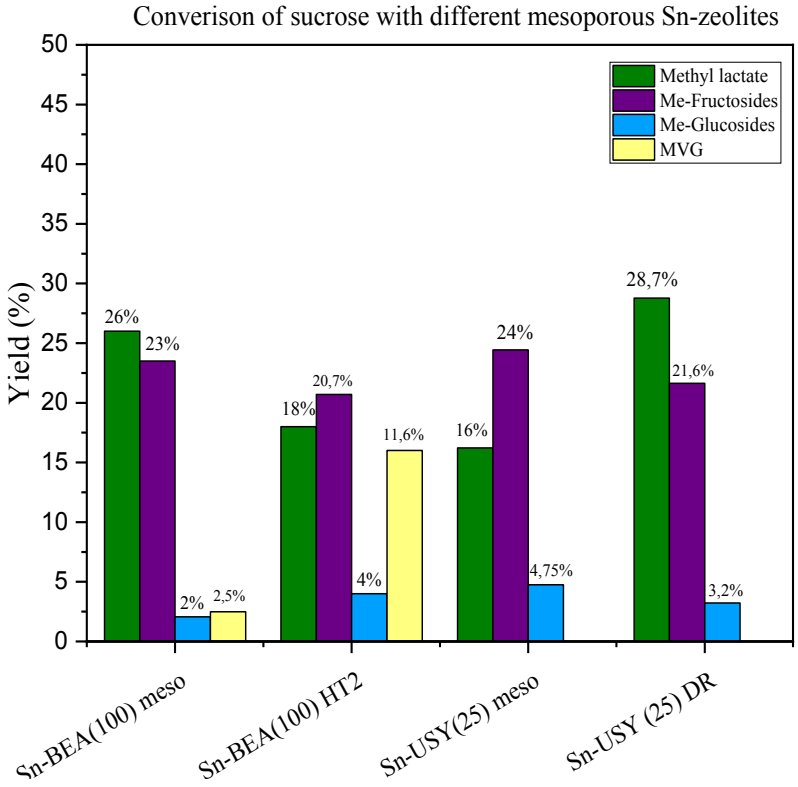

Figure 39: Methyl lactate and co-products percentage of different mesoporous Sn-zeolite when reacting with sucrose

Reaction conditions: 120mg substrate, 50 mg catalyst, 80 µL DMSO, 5mL methanol, 160°C, 2 hours.

Again, the BEA mesoporous form gave positive results: the bigger pores allow a faster diffusion of the substrate to the active site, accelerating the formation of fructose and methyl lactate.

Regarding the mesoporous form of the Sn-USY(25) (histogram 3, figure 38) the same interpretation previously done for inulin was still valid: an increase in yield was expected but, because of the partial collapse of the structure caused by the desilication, the amount of mesopores formed is lower. The function of the zeolite is therefore not reliable and hypothesis about shape selectivity were not done on it.

Better results were obtained for the dissolutiuon-reassembly sample (Sn-USY(25) DR, entry (4 in the figure 39): despite the decrease in crystallinity and consequent formation of undetected compound (probably humins and intermediate from glucose), the highest amount of methyl lactate was reported, in combination with reasonable high amount of methyl-fructosides.

4.5.3 Catalytic tests on cellobiose and maltose

Cellobiose and maltose are both made of two glucose units joined together by a β and α-glycosidic bond respectively.

Solubility tests have been made on these substrates without any catalysts: no dissolution has been reported after treatment at 160°C for 2 hours in the microwave reactor.

However, in acidic media, it was possible to solubilize the sugars and submit the sample to NMR analysis in order to locate the signal in the HSQC spectra.

CELLOBIOSE	ML	Me-Fructosides	Me-Glucosides	Cellobiose unreacted
Sn-BEA(100) Micro 2h	0 %	27 %	4.91 %	61.84 %
Sn-BEA(100) Micro 4h	0 %	47 %	6.75%	41.34 %
Sn-BEA(100) Micro 4h*	0 %	38 %	11.14%	47.25 %
Sn-USY(25) Micro 2h	0 %	28.02 %	13.88 %	43.5 %
Sn-USY(25) Micro 4h	2.99 %	21.27 %	21.56%	21.5 %
Sn-USY(25) Micro 2h**	2.93 %	25.53 %	26.01 %	27 %

Table 9: Methyl lactate and co-products percentage of different microporous Sn-zeolite when reacting with cellobiose .Classic reaction conditions: 120mg substrate, 50 mg catalyst, 80 μL DMSO, 5mL methanol, 160°C, 2 hours.

* Reaction conditions: 120 mg substrate, 50 mg catalyst, 5 mL MeOH, 80 μL DMSO, 4 hours, 180 °C

** Reaction conditions: 120 mg substrate, 120 mg catalyst, 5 mL MeOH, 80 μL DMSO,2 hours, 160 °C

Staring with the BEA zeolite (Table 9, entry 1), it was noticeable that, after the conventional two hours of reaction, there was no evidence of methyl lactate or other hydroxyesters, while a big amount (approximately 62 %) of unreacted cellobiose was detected. In fact, it was already known from literature the difficulties in the hydrolysis of the cellobiose bond [73].

In order to obtain improvements in the conversion of the starting substrate, the reaction time was prolonged to 4 hours but still no formation of methyl lactate was observed. However, the amount of unreacted substrate was reduced of 20%, with a corresponding increase in the percentage of methyl fructosides. This means that the hydrolysis in two glucose units, the isomerization to fructose and the subsequent formation of methyl-fructosides occured, but then the Lewis acid sites were not strong enough to catalyze the last step, the formation of methyl lactate.

Alternatively, an increase in temperature of 20 °C had been applied, running the reaction at 180°C for 4 hours, but no significant improvements were reported.

The same evaluation had been done for the Sn-USY catalyst: after 2 hours of reaction there was no evidence of the formation of methyl lactate, but a comparison with the Sn-BEA showed that more cellobiose had been hydrolyzed (20% less present in solution) and the amount of methyl glucosides was almost tripled probably because of the greater acidity of the USY.

After 4 hours of reaction around 3% of methyl lactate was detected by the 800 MHz NMR; the amount of not hydrolyzed cellobiose was halved but this reflect an increase of methyl glucosides and not fructosides, as desired.

Since previously the reaction at 180°C did not give to any successful results, another variation has been tested: in this case the same amount of substrate and catalyst have been loaded in the reaction for 2 hours.

The same results observed at longer reaction time were found: 3 % yield of ML, parallel decrease in unreacted cellobiose and increase in methyl glucosides. So again this modification was not worthwhile for our purpose.

Even if results were not very promising, cellobiose has been tested also with mesoporous system, in order to examine the possible influence of larger pores in the hydrolysis of β-glycosidic bonds.

CELLOBIOSE	ML	Me-Fructosides	Me-Glucosides	Cellobiose unreacted
Sn-BEA (100) Meso 2h	2.05 %	45.94%	13.24%	32.74%
Sn-USY(25) Meso 2h	2.49 %	23.37 %	6.87%	39.15 %

Table 10: Methyl lactate and co-products percentage of different mesoporous Sn-zeolite when reacting with cellobiose. Classic reaction conditions: 120mg substrate, 50 mg catalyst, 80 μL DMSO, 5mL methanol, 160°C, 2 hours.

Comparing the mesoporous BEA behavior with all the three microporous forms (table 10) , it is evident that the first provided the best results, also compared to the test at 180 °C for 4 hours. Even if the amount of ML was low, the percentage of unreacted cellobiose was halved (from 62 % to 33%), promoting the formation of methyl fructosides (from 38 % to 46%).

It is evident that the presence of mesopores affected positively the hydrolysis of the dimer. The methyl glucosides were formed when Lewis acidity was not enough to promote the fast isomerization between glucose and fructose; in these conditions, the formation of the more stable methyl glucosides due to the residual Brønsted acidity became competitive. However, the higher percentage of methyl fructosides proved that the isomerization occured successfully in the majority of the reactions. A reaction was run with an addition of 10% of water to facilitate the hydrolysis but only a slight increase of methyl lactate was observed, without any significant improvement in the study case.

Regarding the USY framework, the mesoporous system did not show great results, not even in terms of conversion of cellobiose: the same considerations previously done in chapter 4.4.1 and 4.4.2 were still valid.

Catalytic tests on maltose were firstly carried out with the Sn-BEA(100) microporous, in order to investigate its reactivity (table 11).

Due to the presence of the α-glycosidic bond and less H-bonds, maltose resulted easier to hydrolyze with 48% unconverted after 2 hours against 62% of cellobiose. However, no

evidence of methyl lactate was obtained after 2 hours of reaction but only a great amount of methyl fructosides were detected.

In order to combine the effects given by larger pores and longer reaction times, a reaction with the mesoporous Sn-BEA(100) was conducted for 4 hours.

MALTOSE	ML	Me-Fructosides	Me-Glucosides	glucose	fructose	Maltose unreacted
Sn-BEA (100) Micro 2h	0%	27.79%	8.79%	8.02%	6.14%	47.6%
Sn-BEA (100) Meso 4h	7.47%	8.97%	17.90%	2.08%	0.57%	44.18%

Table 11: : Methyl lactate and co-products percentage of different mesoporous Sn-zeolite when reacting with maltose. Classic reaction conditions: 120mg substrate, 50 mg catalyst, 80 µL DMSO, 5mL methanol, 160°C, 2 hours.

Only a little amount of methyl lactate, formed from methyl fructosides in a longer reaction time, was observed. However, the presence of mesopores did not affect significantly neither the hydrolysis nor the conversion of maltose and 44 % was still unreacted. The increase in yield could be attributed only to kinetic equilibrium effects: the amount of methyl fructosides decreased to the benefit of ML due to longer reaction time, but the amount of unreacted maltose was still significant.

4.5.4 Catalytic tests with starch

Starch is the rawest and cheapest starting material that can be found among all the previously reported sugars, therefore it could lead to high added value products. A primary catalytic test has been made on it with the microporous Sn-BEA (100), in order to investigate its conversion.

However, the acidity of the catalyst was not enough to dissolve and hydrolyze the substrate, resulting in inactive systems.

Harsh conditions have been tested (increasing reaction times and temperature) but without any improvement.

5. Conclusion

In this research project, different heterogeneous catalytic systems, both microporous and mesoporous, have been synthesized in order to investigate their activity in the conversion of glucose and bulky substrates, such as oligomers.

In the first part of the project, zeolite with different frameworks were dealuminated, impregnated with Sn and tested as catalysts for the conversion of glucose into methyl lactate, in order to evaluate the influence of different structures to the yields in the products. Among all of the microporous forms the Sn-BEA(100) and Sn-USY(25) showed the best catalytic activity, both in terms of selectivity towards methyl lactate and low formation of by-products (methyl-glucosides and HMF). Their stability was also tested with positive results.

Starting from these considerations, their mesoporous counterparts were synthesized according to different synthesis techniques and submitted to catalytic tests for the conversion of glucose and bulky substrates.

Considering firstly the desilication method only the BEA framework gave positive results with an increased yield in ML. The mesoporosity contribute can be noticed using inulin as starting substrate: in addition to the accelerated dissolution of the substrate, the more accessible sites encouraged the formation of bulky molecules speeding up the reaction rate. The same result was found for the surfactant template Sn-BEA(100), which due to wide BET surface area obtained, yielded to double percentage in ML. Similar results were noticed starting from sucrose an easier access to the active sites in the mesoporous system lead to a higher amount of methyl lactate compared to the microporous forms.

A different behavior was observed for the USY framework. Its microporous form showed better performances with inulin compared to the microporous Sn-BEA(100), probably due to its higher acidity which aids the hydrolysis of the oligomer.

After the desilication treatment a collapse of the structure was observed and it was reflected in a lower yield in methyl lactate and a big amount of by-products starting from all the different

substrates. Better results were obtained with the mesoporus form obtained by surfactant templating and dissolution-reassembly procedures. The XRD spectra showed a partial maintenance of the characteristic structure, hence high yield to methyl lactate was reported. The best results were obtained by the dessolution reassembly synthesis especially with sucrose, which is easier to hydrolyze.

Cellulose and maltose were found to be very difficult to hydrolyze with all the catalysts and, neither with more drastic reaction conditions, they yielded to significant amount of methyl lactate or methyl fuctosides.

Finally, two different routes for the hydrothermal synthesis of mesoporous Beta zeolites without the need of Hydrofluoric acid was performed. The first synthesis yielded to an amorphous and inactive zeolite, while the second route lead to a material with better activity for the conversion of glucose and oligomers. With the prospective of a green hydrothermal synthesis ,this latter catalysts can be employed in future works for investigating the conversion of bulky substrates.

6. Appendix

6.1 Appendix A – XRF data- Si/Al and Si/Sn ratio.

Catalyst	Initial Si/Al	Si/Al after De-Al	Si/Sn
Sn-BEA(100)Micro	19	134.75	102.52
Sn-USY(25)Micro	30	70.15	33.75

Sn-BEA (100) Meso	19	127	129
Sn-USY(25)Meso	30	40.62	39.38
Sn-MOR (25)	6.5	30	6500
Sn-ZSM5(25)	25	47	32
Sn-ZSM5(100)	25	31.5	95
Sn-ZSM5(200)	25	30	243
Sn-USY(25) DR	30	60	52
Sn-BEA_HT2 (100)	--	111.3	95.67

Table A1: List of Si/Al and Si/Sn ratio calculated by XRF analysis. The first column reports the type of catalysts with theoretical Si/Sn ratio value in brackets, while in the fourth the effective ratio that is obtained after impregnation is listed . The second and third columns report the value of Si/Al before and after dealumination respectively.

6.2 Appendix B – NMR spectra

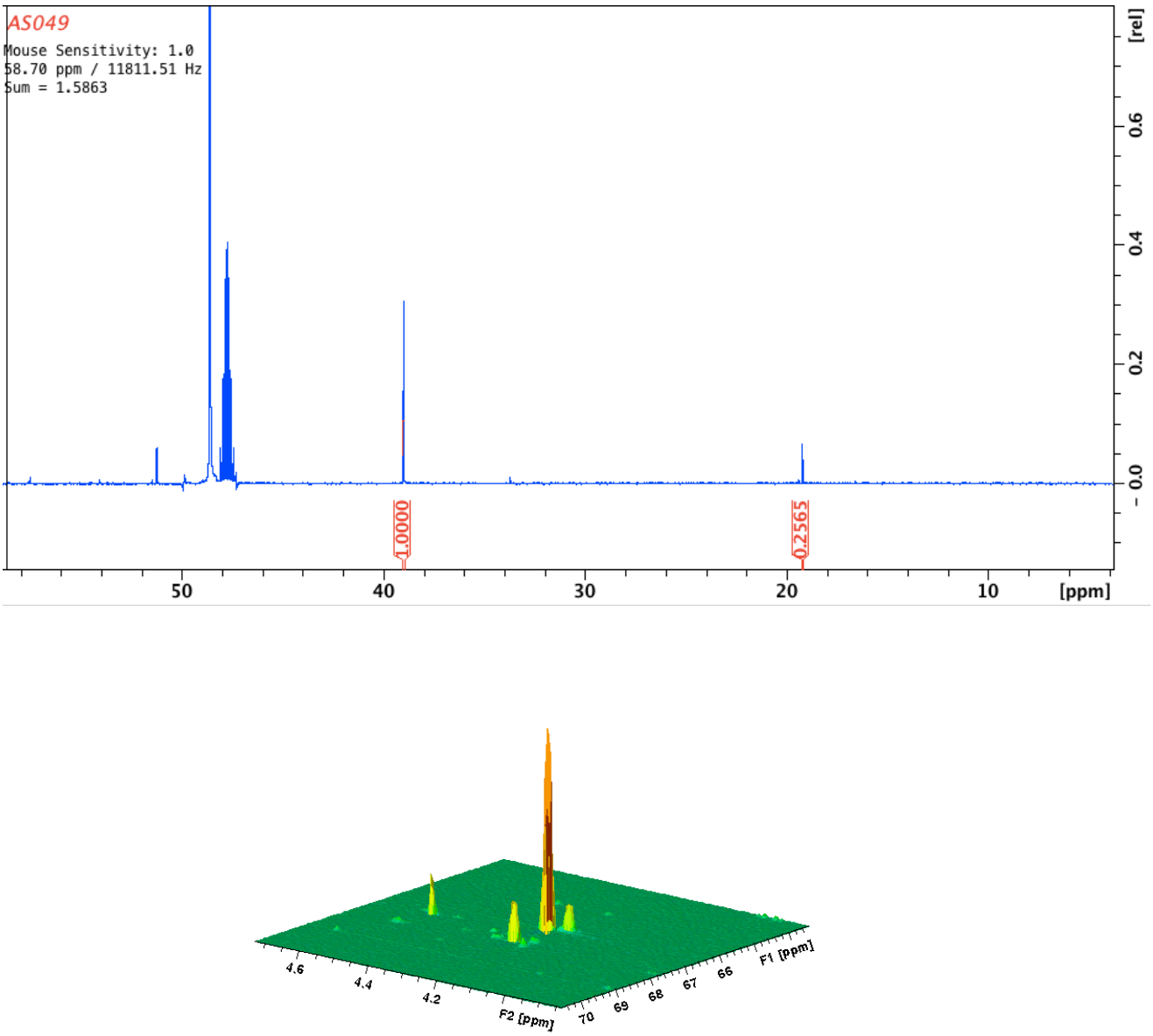

Figure B1: On the top the ^{13}C NMR spectra of reaction of Inulin and water for 2 hours with microporous Sn-BEA(100), 160 °C in MeOH and DMSO as internal standard. The two signals at39 ppm and 19 ppm are DMSO and methyl lactate respectively. Co-products (glyceraldehyde, MVG,THM and furanics) are found at 105 ppm, 112ppm, 135 ppm and 151 ppm. The concentration of methyl lactate is calculated according to the equation reported in chapter 3.3.2. Subsequently is reported the HSQC spectra of the same reaction: the main peak represents the methyl-lactate signal.

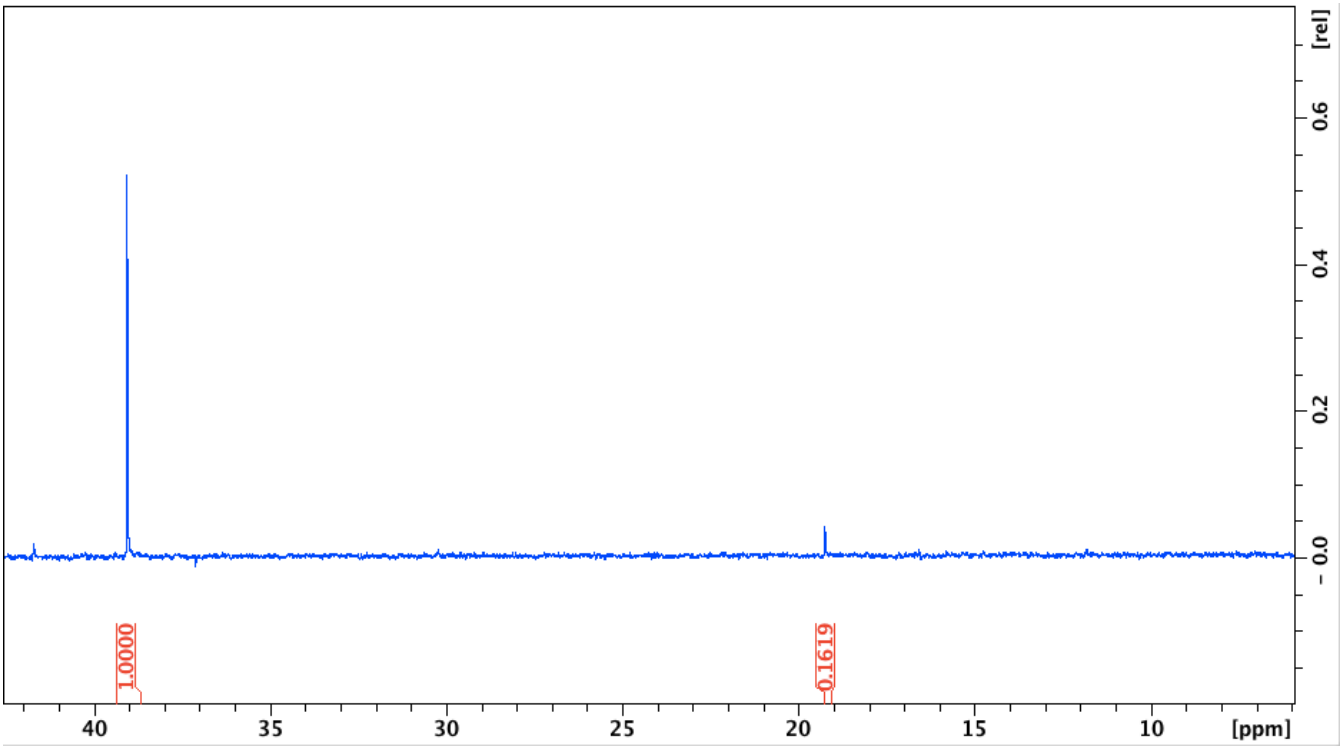

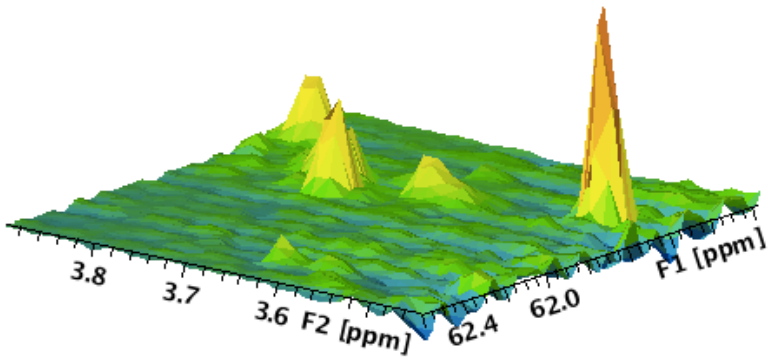

Figure B2: On the top is reported the NMR spectra of the reaction with Sn-USY DR and sucrose for 2 hours at 160°C in MeOH and DMSO as internal standard. The DMSO signal is found at 39 ppm, while the methyl lactate at 19 ppm. Co-products (glyceraldehyde, MVG,THM and furanics) are found at 105 ppm, 112ppm, 135 ppm and 151 ppm respectively. The equation reported in chapter 3.3.2 allowed the obtainement of the concentration of each analyte. The underlying 2D-HSQC diagram shows the main peaks of methyl-glycosides for the same reaction. The quantification was made using the same equation for the ^{13}C integrals.

6.3 Appendix C- SEM pictures

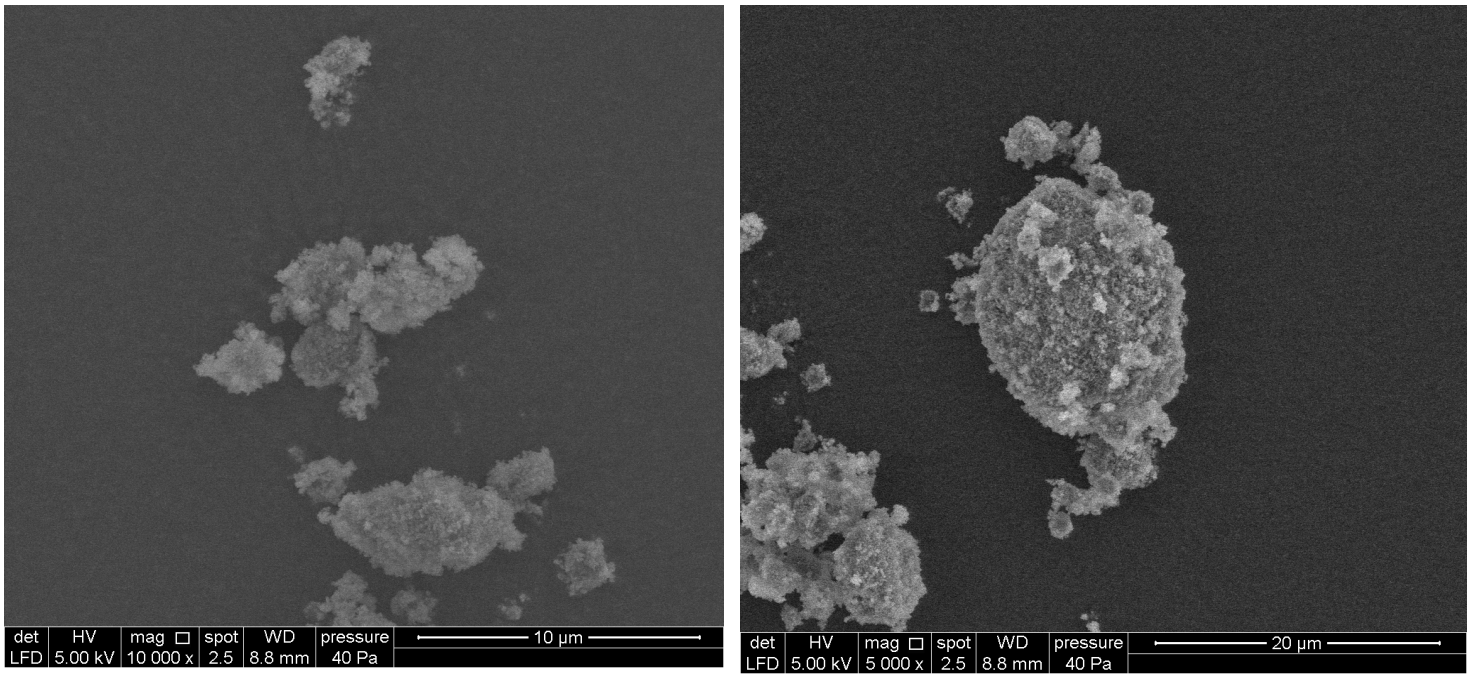

Figure C1: SEM Picture of the zeolite Sn-BEA HT2 (100) obtained by hydrothermal treatment with PDADMA and TEAOH. From the picture is visible the presence of amorphous material which can be significantly reduced with longer reaction time.

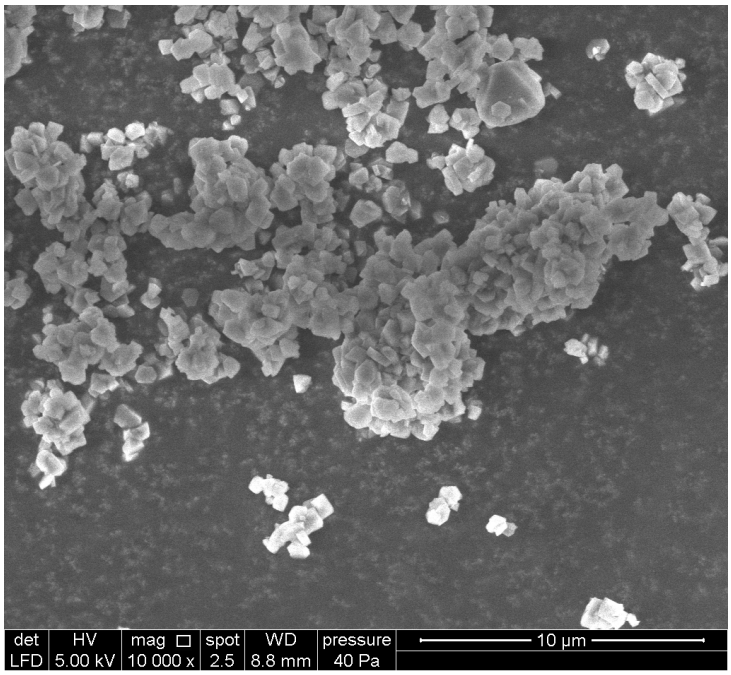

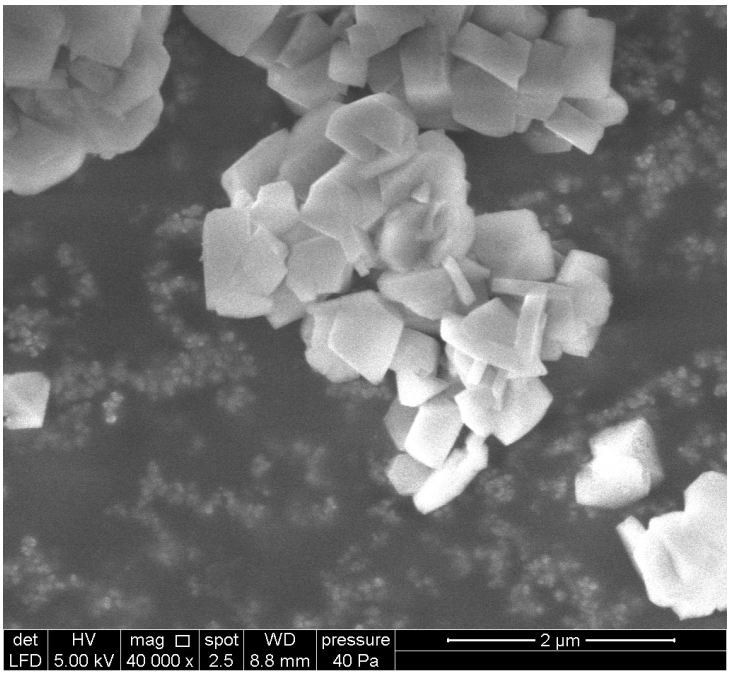

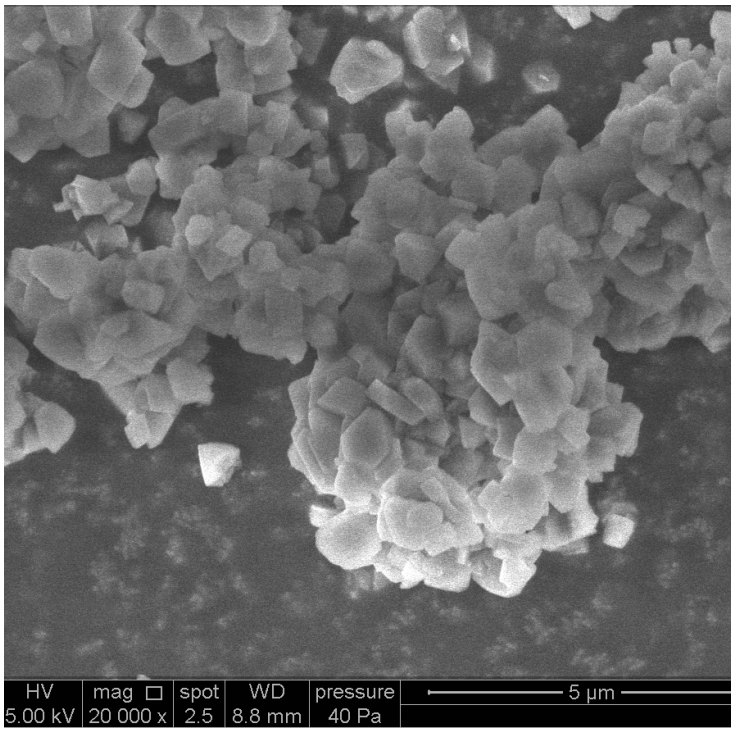

Figure C2 : SEM Pictures of the mesoporous USY zeolite obtained by dessolution and reassembly procedure (Sn-USY_DR). The formation of a crystalline structure was achieved successfully as reported from the XRD difractogram.

7. References

[1] H. Van Bekkum, E. M. Flanigen and J.C. Jansen, Introduction to Zeolite Science and Practice, *Stud*. *Surf. Sci. Catal*., Elsevier Science Publisher , the Netherlands **1991**, vol 58

[2] K. Egeblad, C. H. Christensen, M. Kustova and C. H. Christensen, *Chem. Mater.*, **2008**, *20* (3), pp 946–960.

[3] J.B.Nagy, P.Bodart, I.Hannus, I.Kiricsi, Synthesis, characterization and use of zeolitic microporous materials.*DecaGen Ltd*. **1998**.

[4] N.Y.Chen, W. E. Garwood, F. G. Dwyer, Shape selective catalysis in Industrial applications from *Mobil Research and Development corporation.*

[5] Csicsery, S. M., Shape-selective Catalysis in Zeolites. *Zeolites* **1984**, *4* (3), 202- 213.

[7] S. Tolborg, A. Riisager, I. Sadaba, Synthesis characterization and evaluation of Tin-containing silicates for biomass conversion

[8] Karmen Margeta, Nataša Zabukovec Logar, Mario Šiljeg and Anamarija Farkaš, Natural zeolites in water treatment- How effective is their use

[9] M. Silaghi, C. Chizallet, P. Raybaud, Challenges on molecular aspects of dealumination and desilication of zeolites.

[10] B. Sulikowski, Heterog. *Chem. Rev*., **1996**, 3, 203–268

[11] T. Inui, *Stud. Surf. Sci. Cata*l., **1997**, 105, 1441–1468

[12] C. S. Cundy, *Stud. Surf. Sci. Catal*., **2005**, 157, 65–90

[13] T. Blasco, M.A. Camblor, A. Corma, P. Esteve, J. M. Guil, A. Martinèz, J.A. Perdigòn-Melòn, S. Valencia*, J. Phys. Chem* , **1998**

[14] M. Müller, G. Harvey, R. Prins, *Microporous Mesoporous Mater.* 34 (**2000**) 135-147.

[15] C. Hammond, S. Conrad, and I. Hermans. Simple and Scalable Preparation of Highly Active Lewis Acidic Sn-b. *Angew. Chem.* Int. Ed. **2012**, 51, 11736 –11739

[16] G.T. Kerr,J. *Phys. Chem 71*(**1967**) 4155-4156.

[17] Dijkmans, J.; Demol, J.; Houthoofd, K.; Huang, S.; Pontikes, Y.; Sels, B., Post- synthesis Snβ: An Exploration of Synthesis Parameters and Catalysis. *J. Catal.* **2015**, *330*, 545-557.

[18] Kang, Z.; Liu, H. o.; Zhang, X., Preparation and Characterization of Sn-β Zeolites by a Two-Step Postsynthesis Method and Their Catalytic Performance for Baeyer-Villiger Oxidation of Cyclohexanone. *Chin. J. Catal.* **2012**, *33* (5), 898-904.

[19] Tolborg, S.; Sádaba, I.; Osmundsen, C. M.; Fristrup, P.; Holm, M. S.; Taarning, E., Tin-containing Silicates: Alkali Salts Improve Methyl Lactate Yield from Sugars. *ChemSusChem* **2015**, *8* (4), 613-617.

[20] Li, P.; Liu, G.; Wu, H.; Liu, Y.; Jiang, J.-g.; Wu, P., Postsynthesis and Selective Oxidation Properties of Nanosized Sn-Beta Zeolite. *J. Phys. Chem. C* **2011**, *115* (9), 3663-3670.

[21] van der Graaff, W. N. P.; Li, G.; Mezari, B.; Pidko, E. A.; Hensen, E. J. M., Synthesis of Sn-Beta with Exclusive and High Framework Sn Content. *ChemCatChem* **2015**, *7* (7), 1152-1160.

[23] Tang, B.; Dai, W.; Wu, G.; Guan, N.; Li, L.; Hunger, M., Improved Postsynthesis Strategy to Sn-Beta Zeolites as Lewis Acid Catalysts for the Ring- Opening Hydration of Epoxides. *ACS Catal.* **2014**, *4* (8), 2801-2810.

[24] Hammond, C.; Padovan, D.; Al-Nayili, A.; Wells, P. P.; Gibson, E. K.; Dimitratos, N., Identification of Active and Spectator Sn Sites in Sn-β Following Solid-State Stannation, and Consequences for Lewis Acid Catalysis. *ChemCatChem* **2015**, *7* (20), 3322-3331.

[25] A. Corma, *Chem. Rev*. **1995**. 95, 559-614.

[26] Corma, A.; Iborra, S.; Mifsud, M.; Renz, M., Mesoporous Molecular Sieve Sn- MCM-41 as Baeyer-Villiger Oxidation Catalyst for Sterically Demanding Aromatic and α,β-Unsaturated Aldehydes. *Arkivoc* **2005**, *IX*, 124-132.

[27] D.M. Bibby, R.F.Howe, G.D. McLellan, Coke formation in high-silica zeolites, *Applied Catalysis A:genera*l, 93 (**1992**) 1-34

[28] R. Srivastava, M. Choi and R. Ryoo, *Chem. Commun*., **2006**, 4489–4491

[29] J. Kim, M. Choi and R. Ryoo, *J. Catal.,* **2010**, 269, 219–228

[30] K. Na, C. Jo, J. Kim, K. Cho, J. Jung, Y. Seo, R.J. Messinger, B.F. Chmwlka, R. Ryoo, *science* 2011, 333, 328-332.

[31] Y. Jin, Y. Li, S. Zhao, Z. Lv, Q. Wang, X. Liu, L.Wang, *Microporous Mesoporous Mater*. **2012**, 147, 259-266.

[32] Jian Zhang, Liang Wang, Guoxiong Wang, Fang Chen, Jie Zhu, Chengtao Wang, Chaoqun Bian, Shuxiang Pan, and Feng-Shou Xiao, *ACS Sustainable Chem. Eng*. **2017**,5, 3123-3131.

[35] C.Marcilly , Acido-Basic Catalysis – *Application to Refining the Petrolchemistry, Ed. Technip,* **2005**.

[36] D.A.Young, Y. Linda, *US3326797,* **1967**.

[37] J.C Groen, J.C. Jansen, J.A. Moulijin, J. Perez-Raminez*, J. Phys. Chem. B.* **2004**, 108,13062-13065.

[38] Alexander Sachse, Aida Grau-Atienza, Erika O. Jardim, Noemi Linares, Matthias Thommes and Javier García-Martínez*, Cryst. Growth Des*. **2017**, 17, 4289-4305

[39] Garcia-Martinez,J., Johnson , M., Valla J., Li, K., Ying, J. Y. *Catal.Sci. Technol*. **2012**,2, 987-994.

[40] Y.Goto, Y. Fukushima, P. Ratu, Y. Imada, Y. Kubota, Y. Sugi, M. Ogura, M. Matsukata, J. *Porous Mat.* **2002**, 9, 43-48

[41] I.I.Ivanova, A.S. Kuznetsov, V.V. Yuschenko, E.E: Knyazeva, *Pure Appl. Chem* **2004**, 76, 1647- 1657

[43] Plastics – the Facts 2016, http://www.plasticseurope.org/ Document/plastics---the-facts-2016-15787.aspx, (accessed January 2017).

[44] A. Cózar, F. Echevarría, J. I. González-Gordillo, X. Irigoien, B. Úbeda, S. Hernández-León, Á. T. Palma, S. Navarro, J. García-de-Lomas, A. Ruiz, M. L. Fernández-de-Puelles and C. M. Duarte*, Proc. Natl. Acad. Sci. U. S. A*., **2014**, 111, 10239.

[45] K. L. Law and R. C. Thompson, *Science*, **2014**, 345, 144.

[46] L.C Woodall, A. Sanchez-vidal, G.L.J. Paterson, R. Coppock, V. Sleight, A. Calafat, A. D. Rogers, B.E. Narayanaswamy and R. C. Thompson, *R. Soc. Open Sci.,* **2014**, 1, 1.

[47] A. V. Bridgwater, *Chem. Eng. J.,* **2003**, 91, 87–102.

[48] European Bioplastics, nova-Institute (2017). www.bio-based.eu/markets.

[49] L. Shen, J. Haufe and M. K. Patel, Product overview and market projection of emerging bio-based plastics, Utrecht, **2009**.

[51] M. Pietrini, L. Roes, M.K. Patel and E. Chiellini, *Biomacromolecules*, **2007**,8,2210.

[52] T. Ennaert, J.V: Aelst, J. Dijkmans, R. De Clerq, W. Schutyser, M. Dusselier, D. Verboekend, B. F. Sels, *Chem. Soc. Rev*., **2016**,45,584

[53] F.W. Lichtenthaler, *Acc. Chem. Res.,* **2002**, 35, 728

[54] Sugar: World Markets and trade, United States Department of Agriculture.

[55] M. Shoaib, A. Shehzad, M. Omar, A. Rakha, H. Raza, H. R. Sharif, A. Shakeel, A. Ansari and S. Niazi, *Carbohydr. Polym*., **2016**, 147, 444–454.

[56] T. Barclay, M. Ginic-Markovic, M. R. Johnston, P. D. Cooper and N. Petrovsky, *Carbohydr. Res.,* **2012**, 352, 117–125.

[57] F. A. Castillo Martinez, E. M. Balciunas, J. M. Salgado, J. M. Domínguez González, A. Converti and R. P. S. Oliveira, *Trends Food Sci. Technol*., **2013**, 30, 70.

[58] M. Crank, M. Patel, F. Marscheider-Weidemann, J. Schleich, B. Hüsing and G. Angerer, Techno-economic Feasibility of Large-scale Production of Bio-based Polymers in Europe, Sevilla, **2005**.

[59] Lactic Acid Market Analysis By Application & Polylactic acid (PLA) Market Analysis By Application And Segment Forecasts, 2014–2025, http://www.grandviewresearch.com/industry-analysis/lactic-acid-and-poly-lactic-acid-market, (**accessed January 2017**).

[60] B. Sels and M. Dusselier, WO 2014/122294A1, **2014**.

[61] Taarning, E.; Saravanamurugan, S.; Spangsberg, H. M.; Xiong, J.; West, R. M.; Christensen, C. H., Zeolite-Catalyzed Isomerization of Triose Sugars. *ChemSusChem* **2009**, *2* (7), 625-627.

[62] M. Moliner, Y. Román-Leshkov and M. E. Davis, *Proc. Natl. Acad. Sci*. U. S. A., **2010**, 107, 6164.

[63] C. M. Lew, N. Rajabbeigi and M. Tsapatsis, *Microporous Mesoporous Mater.,* **2012**, 153, 5

[64] M. Spangsberg Holm, S. Saravanamurugan, E. Taarning , *Conversion of Sugars to Lactic Acid Derivatives Using Heterogeneous Zeotype Catalysts*

[65] I. Tosi, A. Riisager, E. Taarning, P.R. Jensesn, S. Meier, *Cat. Sci.* Technology, DOI: 10.1039/c8cy00335a

[66] D. Padovan, S. Tolborg, L. Botti, E. Taarning, I. Sàdaba, C. Hammond. *React. Chem. Eng*., **2018**, 3, 155.

[67] S. Tolborg, S. Meier, I. Sàdaba, S. G. Elliot, S.K. Kristenesen, S. Saravanamurugan, A. Riisager, T. Skrydstrup, E. Taarning, *Green Chemistry*, DOI: 10.1039/c5gc02840j

[68] Abbas Al-Nayili, Keiko Yakabi and Ceri Hammond , J. *Mater. Chem*. A, **2016**, 4, 1373

[69] L. Wang, Z. Zhang, C. Yin, Z. Shan, F. Xiao, Hierarchical mesopores zeolites with controllable mesoporosity templated from cationic polymers, *micromeso j.*

[70] T. Rundlöfa, M. Mathiassona, S. Bekiroglub, B.Hakkarainena, T. Bowdenc, T. Arvidssona, Survey and qualification of internal standards for quantification by 1H NMR spectroscopy

[71] Samuel G. Elliot, S. Tolborg, I. Sàdaba, E. Taarning, S. Meier, *ChemSusChem* DOI:10.1002/cssc.201700587

[72] A. Ertan, İzmir Institute of Technology İzmir, Turkey , CO2, N2 and Ar Adsorption on Zeolites

[73] C. Moreau, R. Durand, J. Duhamet, P. Rivalier, Hydrolysis of fructose and glucose precursors in the presence of H-form zeolites.

8. Acknowledgements

A first, important thanks goes to the Professor Fabrizio Cavani ,who not only made me work for few months in his research group in Bologna, but also made possible my aborad traineeship in Denmark, finding a suitable project and exchange program at the DTU.

Right after there is the PhD student Irene Tosi, who with infinity patience lead me in the laboratory work and helped me with any doubts and requests. She also always made sure to make me feel confortable and settled in, in a foreign country. Thanks also to the professor Andres Riisager : he allowed me to work in his research group at the Sustainable Chemistry Centre at the Denmark Tekniske Universitet, Lyngby, Denmark.

I would like to thank also my parents, they always support my decisions and wanted the best for me, being always present with a heartening word from home.

Last but not least there are friends: friends of a life and friends I met in Denmark. All of them made this last years of university unforgettable and full of emotions.